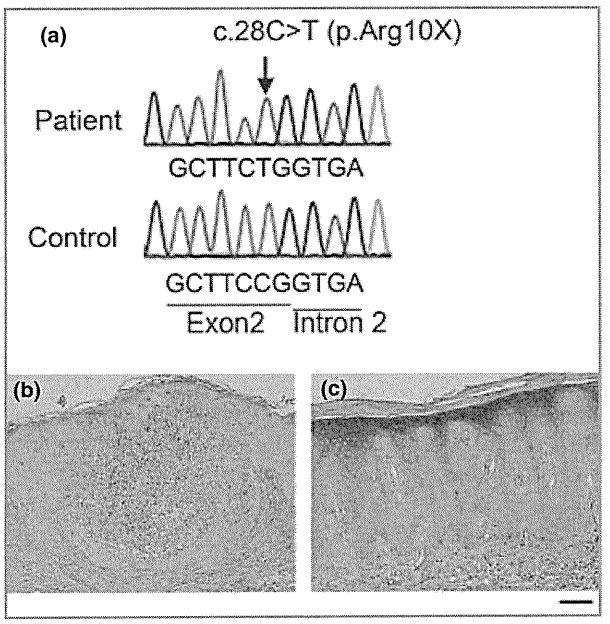

Fig 2. Sequence data of *IL36RN* and expression of IL36RN on the lesion of generalized pustular psoriasis (GPP). (a) Sequence data of *IL36RN* in the patient and control; the arrow indicates the heterozygous mutation c.28C>T (p.Arg10Ter). C at nucleotide position 28 is two bases upstream from the C′ end of exon 2 (the exon 2–intron 2 boundary) of *IL36RN*. (b) Immunohistochemistry of the GPP lesion with anti-IL1F5 (IL36RN); staining was almost negative. (c) Immunohistochemistry of a skin lesion of a patient with psoriasis vulgaris with anti-IL1F5 (IL36RN); staining was strong in keratinocytes in the upper layers. Scale bar = 100 μm.

In addition, it is noteworthy that no GPP cases with *IL36RN* mutations, including the present case, have been associated with PV or PPP,[1,2] and the absence of PV and PPP is a clue in identifying patients with GPP with *IL36RN* mutations.

We believe it is very important to discriminate familial GPP cases with *IL36RN* mutations from the other GPP cases, not only for genetic counselling but also because we expect familial GPP will be treatable with customized therapy that targets IL-36 signalling in the near future.

Departments of [1]*Dermatology,* [3]*Laboratory Medicine, Nagoya University Graduate School of Medicine, 65 Tsurumai-cho, Showa-ku, Nagoya 466-8550, Japan*
[2]*Department of Dermatology, Inazawa City Hospital, 1-1 Gokusho-cho, Inazawa 492-8510, Japan*
E-mail: kazusugi@med.nagoya-u.ac.jp

K. SUGIURA[1]
T. TAKEICHI[1,2]
M. KONO[1]
Y. OGAWA[1]
Y. SHIMOYAMA[3]
Y. MURO[1]
M. AKIYAMA[1]

References

1 Marrakchi S, Guigue P, Renshaw BR *et al.* Interleukin-36-receptor antagonist deficiency and generalized pustular psoriasis. *N Engl J Med* 2011; **365**:620–8.
2 Onoufriadis A, Simpson MA, Pink AE *et al.* Mutations in IL36RN/IL1F5 are associated with the severe episodic inflammatory skin disease known as generalized pustular psoriasis. *Am J Hum Genet* 2011; **89**:432–7.
3 Mulero JJ, Pace AM, Nelken ST *et al.* IL1HY1: a novel interleukin-1 receptor antagonist gene. *Biochem Biophys Res Commun* 1999; **263**:702–6.
4 Smith DE, Renshaw BR, Ketchem RR *et al.* Four new members expand the interleukin-1 superfamily. *J Biol Chem* 2000; **275**:1169–75.
5 Dinarello C, Arend W, Sims J *et al.* IL-1 family nomenclature. *Nat Immunol* 2010; **11**:973.
6 Debets R, Timans JC, Homey B *et al.* Two novel IL-1 family members, IL-1 delta and IL-1 epsilon, function as an antagonist and agonist of NF-kappa B activation through the orphan IL-1 receptor-related protein 2. *J Immunol* 2001; **167**:1440–6.
7 Towne JE, Garka KE, Renshaw BR *et al.* Interleukin (IL)-1F6, IL-1F8, and IL-1F9 signal through IL-1Rrp2 and IL-1RAcP to activate the pathway leading to NF-kappaB and MAPKs. *J Biol Chem* 2004; **279**:13677–88.
8 Sahashi K, Masuda A, Matsuura T *et al. In vitro* and *in silico* analysis reveals an efficient algorithm to predict the splicing consequences of mutations at the 5′ splice sites. *Nucleic Acids Res* 2007; **35**:5995–6003.
9 Blumberg H, Dinh H, Trueblood ES *et al.* Opposing activities of two novel members of the IL-1 ligand family regulate skin inflammation. *J Exp Med* 2007; **204**:2603–14.

Funding sources: this study was supported in part by a Grant-In-Aid for Scientific Research, (C) 23591617 (to K.S.) and (A) 23249058 (to M.A.) from the Ministry of Education, Culture, Sports, Science and Technology of Japan.

Conflicts of interest: none declared.

The utility of the 'book biopsy' in Mohs micrographic surgery

DOI: 10.1111/j.1365-2133.2012.10967.x

MADAM, By virtue of its tissue-sparing properties and enabling assessment of 100% of the surgical margin, Mohs micrographic surgery (MMS) is considered the gold standard in the surgical treatment of high-risk facial skin cancer.[1–3] Clinicians may often initially perform diagnostic biopsies to confirm the diagnosis (if doubt exists) and also to enable histopathological assessment of any high-risk features such as an infiltrative growth pattern or the presence of perineural invasion.

In order to guide the size of the first Mohs layer, the surgeon typically marks out the clinical extent of the tumour on the skin. However, in patients with significant actinic damage, it may be very difficult clinically to determine the tumour margins. Overestimating the clinical extent of the tumour will result in a surgical defect larger than required; however, not including 'suspicious' areas may result in several stages of surgery, a longer procedure for the patient and an increase in the tissue-processing burden for the Mohs laboratory technicians.

Under such circumstances the 'book biopsy' (BB) may be of value. Figure 1 illustrates the preoperative appearance of a 69-year-old man with a biopsy-proven infiltrating basal cell carcinoma on the lower left nasal dorsum. A previous inci-

The β9 Loop Domain of PA-PLA$_1$α Has a Crucial Role in Autosomal Recessive Woolly Hair/Hypotrichosis

Journal of Investigative Dermatology (2012) **132,** 2093–2095; doi:10.1038/jid.2012.96; published online 5 April 2012

TO THE EDITOR

Membrane-associated phosphatidic acid–preferring phospholipase A$_1$α (PA-PLA$_1$α, also known as mPA-PLA$_1$α and lipase H (LIPH)) is an enzyme known to hydrolyze phosphatidic acid (PA) into 2-acyl lysophosphatidic acid (LPA) and free fatty acid (FFA; Sonoda *et al.*, 2002; Hiramatsu *et al.*, 2003). It has recently been shown that LPA, which is produced by PA-PLA$_1$α, works as a ligand for its receptor LPA$_6$, also known as P2Y5, and is speculated to regulate the proliferation and differentiation of inner root sheath cells of hair follicles (Inoue *et al.*, 2011). Recently, *LIPH* (MIM# 607365) and *LPAR6* (MIM# 609239), which encode PA-PLA$_1$α and LPA$_6$, respectively, were identified as causative genes for autosomal recessive woolly hair with associated hypotrichosis (ARWH/H; MIM# 604379, 278150; Kazantseva *et al.*, 2006; Pasternack *et al.*, 2008; Shimomura *et al.*, 2008). To our knowledge, we identified a previously unreported heterozygous missense mutation at the β9 loop domain of PA-PLA$_1$α, which is considered a crucial structure for substrate recognition (Sonoda *et al.*, 2002; Aoki *et al.*, 2007) in this study. To clarify the role of the β9 loop domain, the hydrolytic activity and LPA$_6$ activation ability of mutant PA-PLA$_1$α were evaluated.

A 3-year-old Japanese girl was seen at our hospital with woolly and sparse hair on her scalp without other abnormalities (Figure 1a). Her eyebrows and eyelashes were slightly sparse. Her parents were unrelated and nonconsanguineous, and had normal hair. Blood samples were collected for DNA extraction in accordance with standard methods, and an *LIPH* mutation search was performed as previously reported (Shimomura *et al.*, 2009). Direct sequencing analysis of all exons and intron–exon boundaries of the *LIPH* revealed that the patient was compound heterozygous for the two missense mutations c.619G>C (p.Asp207His)

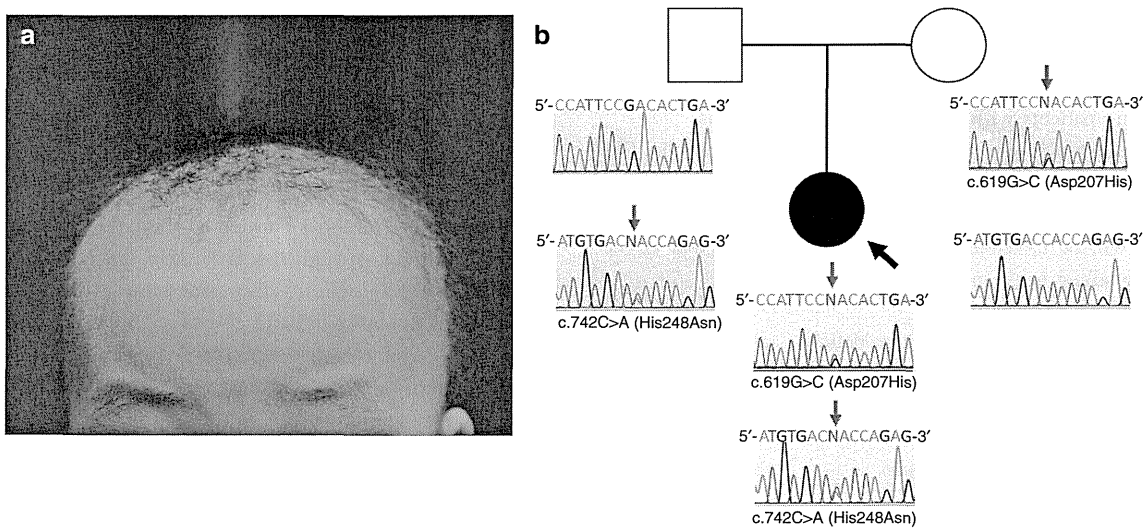

Figure 1. Clinical features and identification of mutations in the *LIPH* gene. (**a**) The affected individual has features of autosomal recessive woolly hair/hypotrichosis, which is characterized by sparse woolly hair on the scalp and slightly sparse eyebrows and eyelashes. There are no other abnormalities. (**b**) Family pedigree. The family history is consistent with autosomal recessive inheritance. Direct sequencing of the *LIPH* gene revealed that the patient had compound heterozygous missense mutations involving c.619G>C and c.742C>A. The complementary DNA (cDNA) nucleotides and the amino acids of the protein were numbered based on the previous sequence information (GenBank accession number; AY093498.1). Nucleotide numbering reflects cDNA numbering, with +1 corresponding to the A of the ATG translation initiation codon in the reference sequence, according to Human Genome Variation Society guidelines (www.hgvs.org/mutnomen). The initiation codon is codon 1.

Abbreviations: a.a., amino acid; AP-TGFα, alkaline phosphatase–tagged transforming growth factor-α; FFA, free fatty acid; LPA, lysophosphatidic acid; PA, phosphatidic acid; PA-PLA$_1$α, membrane-associated phosphatidic acid–preferring phospholipase A$_1$α; PLA$_1$, phospholipase A$_1$; PS, phosphatidylserine; PS-PLA$_1$, phosphatidylserine-specific phospholipase A$_1$; TG, triacylglycerol; WT, wild type

and c.742C>A (p.His248Asn), which were segregated from her mother and father, respectively (Figure 1b). These mutations were verified by restriction enzyme digestions of the PCR products by *Hpy*188I and mutant allele-specific amplification analysis, respectively (Supplementary Figure S1 online). p.His248Asn, one amino acid (a.a.) of the catalytic triad, is known as a prevalent pathogenic mutation in the Japanese population (Shinkuma *et al.*, 2010).

To the best of our knowledge, c.619G>C (p.Asp207His) in *LIPH* is a previously unreported mutation and was not found in alleles from 100 normal unrelated individuals. Asp^{207} residue of PA-PLA$_1$α is conserved among diverse species, suggesting that Asp^{207} may have a critical role in enzyme activity (Supplementary Figure 2a online). To assess the role of Asp^{207} as a candidate for the ARWH/H, two distinct *in vitro* functional analyses were performed: for hydrolytic activity and for LPA$_6$ activation ability of PA-PLA$_1$α (Shinkuma *et al.*, 2010).

To investigate the molecular defects underlying the mutation, we synthesized p.Asp207His PA-PLA$_1$α expression constructs and compared the mutant protein expression with wild-type (WT) and with p.Ser154Ala, which was known as a loss-of-function mutation (Shinkuma *et al.*, 2010; Sonoda *et al.*, 2002). Immunoblot analysis using anti-PA-PLA$_1$α monoclonal antibody revealed that the transfection of p.Asp207His constructs into HEK293 cells resulted in the secretion of the 55-kDa mutant PA-PLA$_1$α at levels similar to those of WT and p.Ser154Ala (Figure 2a; Sonoda *et al.*, 2002). In addition, the same amounts of mutant PA-PLA$_1$α proteins were also recovered from the cell lysate (data not shown). These results indicate that there was no significant difference in protein amount between WT and mutant PA-PLA$_1$α.

Hydrolysis activity was determined by measuring FFA, which was concurrently produced from PA by PA-PLA$_1$α. Briefly, we added the supernatant from HEK293 cells transfected with WT, p.Ser154Ala, or p.Asp207His PA-PLA$_1$α to a medium containing 400 μM PA. After 3 hours of incubation at 37 °C, the amount of oleic acids, one kind

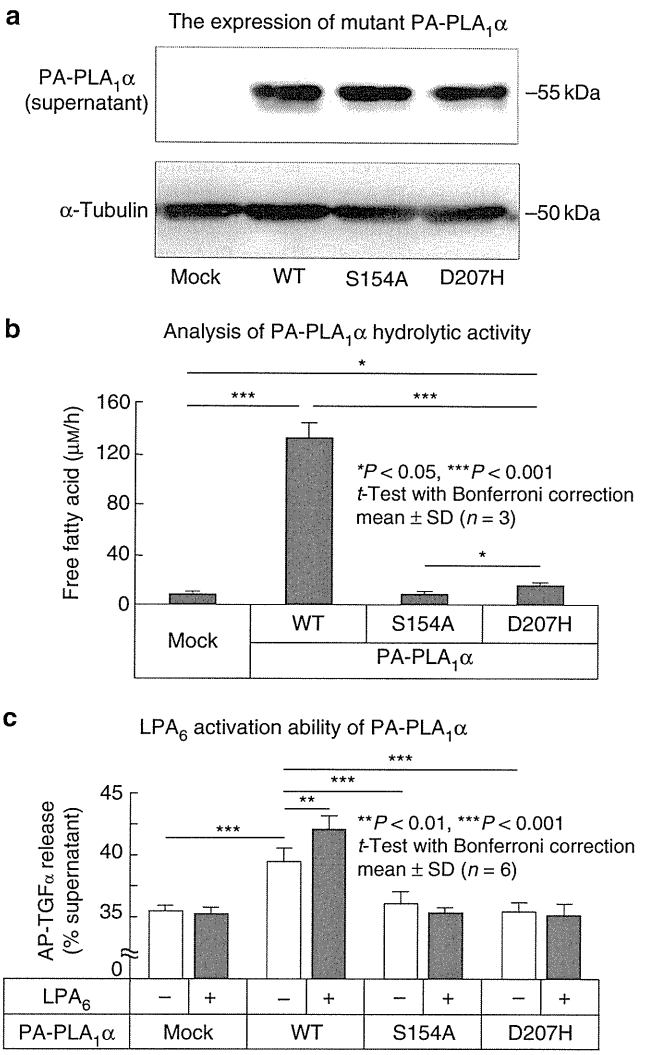

Figure 2. Hydrolytic activity and LPA$_6$ activation ability of p.Asp207His mutant membrane-associated phosphatidic acid-preferring phospholipase A$_1$α (PA-PLA$_1$α). (**a**) Expression of p.Asp207His mutant PA-PLA$_1$α in HEK 293 cells. HEK 293 cells were transfected with wild-type (WT), p.Ser154Ala (S154A), and p.Asp207His (D207H) *LIPH* cDNA, and the expression levels of PA-PLA$_1$α protein derived from the constructs in cell culture supernatant (upper panel) were compared. There were no significant differences in PA-PLA$_1$α protein expression levels among cells transfected with WT, S154A, and D207H. α-Tubulin expression was used as a standard for assessing the total amount of proteins from cell lysate (lower panel). (**b**) As PA-PLA$_1$α hydrolyzes the free fatty acid (FFA) from phosphatidic acid (PA), we monitored the levels of FFA to determine whether there were differences in PA-PLA$_1$α hydrolytic activity between the WT and each of the two mutants of PA-PLA$_1$α. After 3 hours of incubation of the supernatant from HEK293 cells expressing WT, S154A, or D207H PA-PLA$_1$α, with a medium including 400 μM PA, the levels of FFA hydrolyzed by D207H mutant PA-PLA$_1$α were significantly lower than those hydrolyzed by WT PA-PLA$_1$α; however, the D207H PA-PLA$_1$α slightly retained the function of hydrolytic activity compared with control S154A mutant and the empty vector (mock). WT = P<0.001 and D207H = P<0.05 versus mock; D207H = P<0.001 versus WT (one-way analysis of variance (ANOVA) with Dunnett's post test). (**c**) To monitor LPA$_6$ activation level by mutant and WT PA-PLA$_1$α, we used *p*-nitrophenyl phosphate as a substrate for cleavage of alkaline phosphatase-tagged transforming growth factor-α (AP-TGFα) and measured the amount of AP-TGFα released from the HEK293 cells. The amount of free AP-TGFα produced by LPA$_6$ mock-transfected (LPA$_6^-$) cells that were also transfected with WT PA-PLA$_1$α was significantly greater than that produced by LPA$_6^-$ cells transfected with an empty vector (mock PA-PLA$_1$α). This indicates that HEK293 cells act to shed AP-TGFα, an activity that might be mediated by intrinsic LPA receptors. The amounts of AP-TGFα released from LPA$_6$-transfected (LPA$_6^+$) cells expressing S154A or D207H mutant PA-PLA$_1$α and LPA$_6^+$ cells transfected with an empty vector (mock) are significantly lower than those released from LPA$_6^+$ cells expressing WT PA-PLA$_1$α. WT = P<0.001, S154A = not significant (NS) and D207H = NS versus mock (one-way ANOVA with Dunnett's post test).

of FFA, was measured using a NEFA C-Test Wako test kit (Wako Chemicals, Osaka, Japan; Shinkuma *et al.*, 2010). The quantities of oleic acids produced by the p.Asp207His PA-PLA$_1$α were markedly lower than those for the WT; however, the p.Asp207His PA-PLA$_1$α slightly retained the function of hydrolytic activity relative to mock and p.Ser154Ala (Figure 2b).

To perform the LPA$_6$ activation ability assay, alkaline phosphatase–tagged transforming growth factor-α (AP-TGFα; kindly provided by Dr Higashiyama, Ehime University, Japan; Tokumaru *et al.*, 2000), recombinant LPA$_6$, and PA-PLA$_1$α constructs (WT, p.Ser154Ala or p.Asp207His) were cotransfected to HEK293 cells. To measure the LPA$_6$ activation potency of mutant PA-PLA$_1$α, AP-TGFα release into conditioned media via a disintegrin and metalloprotease, which was triggered by the activation of LPA$_6$, was quantified using *p*-NPP as a substrate for AP (Shinkuma *et al.*, 2010; Inoue *et al.*, 2011). As previously reported, the free AP-TGFα from the LPA$_6$-untransfected (LPA$_6^-$) cells expressing the WT PA-PLA$_1$α was more abundant than that from the LPA$_6^-$ cells transfected with mock PA-PLA$_1$α, which indicated that the HEK293 cells had the ability to shed AP-TGFα mediated by intrinsic LPA receptor at some level (Figure 2c; Shinkuma *et al.*, 2010; Inoue *et al.*, 2011). AP-TGFα release from LPA$_6$-transfected (LPA$_6^+$) cells expressing the WT PA-PLA$_1$α was remarkably increased compared with mock or mutant PA-PLA$_1$α. There were no significant differences between the data obtained with cells expressing the mutant and mock PA-PLA$_1$α (Figure 2c). These data indicate that the p.Asp207His PA-PLA$_1$α results in the complete loss of LPA$_6$ activation activity. Despite the remaining slight hydrolytic activity, there was complete loss of LPA$_6$ activation ability and no significant difference in clinical features between this patient and other patients with *LIPH* mutations who were revealed as having complete loss of hydrolytic activity (Shinkuma *et al.*, 2010). These findings suggest that the p.Asp207His PA-PLA$_1$α retained slight hydrolytic activity, which was insufficient to activate LPA$_6$ and possibly leading to woolly hair.

Phospholipase A$_1$ (PLA$_1$) is an enzyme that hydrolyzes ester bonds of phospholipids (Aoki, 2004). PLA$_1$, such as phosphatidylserine (PS)-specific PLA$_1$ (PS-PLA$_1$), PA-PLA$_1$α, and PA-PLA$_1$β, form a subfamily in the pancreatic lipase gene family (Sato *et al.*, 1997; Sonoda *et al.*, 2002; Hiramatsu *et al.*, 2003). These PLA$_1$ enzymes distinctly differ from other lipases in that PLA$_1$ enzymes do not hydrolyze triacylglycerol (TG) and that they show strict substrate specificities and act specifically on PS and PA, respectively (Sato *et al.*, 1997; Sonoda *et al.*, 2002; Hiramatsu *et al.*, 2003). The lipase family has three a.a. residues that form the putative catalytic triad and has three surface loops called the lid, the β5 loop, and the β9 loop that cover the active site (Winkler *et al.*, 1990; Carriere *et al.*, 1998; Aoki *et al.*, 2007). A comparison of the a.a. sequences of PLA$_1$ and TG lipases, such as pancreatic lipase and lipoprotein lipase, revealed that PLA$_1$ enzymes have shorter lid and β9 loop than TG lipases (PLA$_1$: 12 a.a. and 13 a.a.; TG lipases: 22–23 a.a. and 18–19 a.a., respectively; Supplementary Figure 2b online; Aoki *et al.*, 2007). Therefore, the lid, the β5 loop, and the β9 loop are implicated in substrate specificity. In this study, we identified the p.Asp207His mutation at the β9-loop domain of PA-PLA$_1$α in the ARWH/H patient, and clarified that the mutant showed substantial abolition of hydrolytic activity and had no LPA$_6$ activation ability. These results confirm that the β9-loop domain of PA-PLA$_1$α has a crucial role in enzyme activity.

CONFLICT OF INTEREST

The authors state no conflict of interest.

ACKNOWLEDGMENTS

We thank the patient and her parents for their generous cooperation and Ms Junko Tamba and Ms Yui Saito for their technical assistance. The family gave written informed consent. The medical ethics committee of Hokkaido University approved all the described studies. The study was conducted according to the Declaration of Helsinki Principles. This work was supported by the Naito Foundation.

Satoru Shinkuma[1], Asuka Inoue[2], Junken Aoki[2], Wataru Nishie[1], Ken Natsuga[1], Hideyuki Ujiie[1], Toshifumi Nomura[1], Riichiro Abe[1], Masashi Akiyama[1,3] and Hiroshi Shimizu[1]

[1]Department of Dermatology, Hokkaido University Graduate School of Medicine, Sapporo, Japan; [2]Graduate School of Pharmaceutical Sciences, Tohoku University, Sendai, Japan and [3]Department of Dermatology, Nagoya University Graduate School of Medicine, Nagoya, Japan
E-mail: qxfjc346@ybb.ne.jp

SUPPLEMENTARY MATERIAL

Supplementary material is linked to the online version of the paper at http://www.nature.com/jid

REFERENCES

Aoki J (2004) Mechanisms of lysophosphatidic acid production. *Semin Cell Dev Biol* 15:477–89

Aoki J, Inoue A, Makide K *et al.* (2007) Structure and function of extracellular phospholipase A1 belonging to the pancreatic lipase gene family. *Biochimie* 89:197–204

Carriere F, Withers-Martinez C, van Tilbeurgh H *et al.* (1998) Structural basis for the substrate selectivity of pancreatic lipases and some related proteins. *Biochim Biophys Acta* 1376:417–32

Hiramatsu T, Sonoda H, Takanezawa Y *et al.* (2003) Biochemical and molecular characterization of two phosphatidic acid-selective phospholipase A1s, mPA-PLA1alpha and mPA-PLA1beta. *J Biol Chem* 278:49438–47

Inoue A, Arima N, Ishiguro J *et al.* (2011) LPA-producing enzyme PA-PLA(1)α regulates hair follicle development by modulating EGFR signalling. *EMBO J* 30:4248–60

Kazantseva A, Goltsov A, Zinchenko R *et al.* (2006) Human hair growth deficiency is linked to a genetic defect in the phospholipase gene LIPH. *Science* 314:982–5

Pasternack SM, von Kugelgen I, Aboud KA *et al.* (2008) G protein-coupled receptor P2Y5 and its ligand LPA are involved in maintenance of human hair growth. *Nat Genet* 40:329–34

Sato T, Aoki J, Nagai Y *et al.* (1997) Serine phospholipid-specific phospholipase A that is secreted from activated platelets. A new member of the lipase family. *J Biol Chem* 272:2192–8

Shimomura Y, Wajid M, Ishii Y *et al.* (2008) Disruption of P2RY5, an orphan G protein-coupled receptor, underlies autosomal recessive woolly hair. *Nat Genet* 40:335–9

Shimomura Y, Wajid M, Petukhova L *et al.* (2009) Mutations in the lipase H gene underlie autosomal recessive woolly hair/hypotrichosis. *J Invest Dermatol* 129:622–8

Shinkuma S, Akiyama M, Inoue A *et al.* (2010) Prevalent LIPH founder mutations lead to loss of P2Y5 activation ability of PA-PLA1alpha in autosomal recessive hypotrichosis. *Hum Mutat* 31:602–10

Sonoda H, Aoki J, Hiramatsu T *et al.* (2002) A novel phosphatidic acid-selective phospholipase A1 that produces lysophosphatidic acid. *J Biol Chem* 277:34254–63

Tokumaru S, Higashiyama S, Endo T *et al.* (2000) Ectodomain shedding of epidermal growth factor receptor ligands is required for keratinocyte migration in cutaneous wound healing. *J Cell Biol* 151:209–20

Winkler FK, D'Arcy A, Hunziker W (1990) Structure of human pancreatic lipase. *Nature* 343:771–4

excrescence where it is distal in subungual exostosis and not related to the metaphyseal area, whereas in subungual osteochondroma it is in proximity with the metaphyseal area. Also, the cap is composed of fibrocartilage in exostosis and of hyaline cartilage in osteochondromas.[3]

The anatomic singularities of the nail unit explain why bony tumors and osseous outgrowths of the distal phalanx quickly interfere with the nail apparatus.[5] Our patient showed typical features of subungual osteochondroma that reached this large size. The tumor compressed the nail bed and displaced its protective plate away thus exposing the bed to the external environment, which may account for the repeated episodes of bleeding that our patient exhibited.

Mohamed Hussein Medhat El-Komy, MD,[a] Mona Rabie Abdel-Halim, MD,[a] Eman Ahmed El-Nabarawy, MD,[a] Seham El-Tobshy, MSc,[c] Suzan Shalaby, MSc,[a] and Ayman Ismail Kamel, MD[b]

Departments of Dermatology[a] and Radiology,[b] Faculty of Medicine, and Student's Hospital,[c] Cairo University, Egypt

Funding sources: None.

Conflicts of interest: None declared.

Correspondence to: Mohamed Hussein Medhat El-Komy, MD, 5 Falaky Square, Bab El-Louk, Cairo, Egypt.

E-mail: komy_m@yahoo.com

REFERENCES

1. Rottgers SA, Rao G, Wollstein R. Subungual extraosseous chondroma in a finger. Am J Orthop 2008;37:E187-90.
2. Vázquez-Flores H, Domínguez-Cherit J, Vega-Memije ME, Sáez-De-Ocariz M. Subungual osteochondroma: clinical and radiologic features and treatment. Dermatol Surg 2004;30:1031-4.
3. Schulze KE, Hebert AA. Diagnostic features, differential diagnosis, and treatment of subungual osteochondroma. Pediatr Dermatol 1994;11:39-41.
4. Davis DA, Cohen PR. Subungual exostosis: case report and review of the literature. Pediatr Dermatol 1996;13:212-8.
5. Dumontier CA, Abimelec P. Nail unit enchondromas and osteochondromas: a surgical approach. Dermatol Surg 2001;27:274-9.

http://dx.doi.org/10.1016/j.jaad.2012.04.033

Extraordinarily large protruding accessory breast cancer in a man

To the Editor: Accessory breasts may appear at any point along the milk line from the axilla to the groin, with the commonest location being the axilla.[1] The incidence of accessory breasts varies between 0.6% and 6% in women of various ethnic groups, and the highest prevalence is in the Japanese population.[2]

Fig 1. Accessory breast cancer in male patient. There is protruding dark reddish hard mass in left axilla.

The incidence in Japanese men is one third of that in Japanese women. Cancer originating from accessory breast tissue has been reported to account for 0.3% to 0.6% of all breast cancers.[3] Primary carcinoma in accessory breasts in men is extremely rare.

A 73-year-old Japanese man was referred to our outpatient clinic for the treatment of a tumor on the left axilla. He had noticed an elastic, hard nodule in the left axillary area about 30 years previously. On examination, he was found to have an 8- × 6- × 7-cm dark reddish protruding hard mass with an irregular surface in the left axilla and a 6- × 5-cm immobile subcutaneous mass proximal to it (Fig 1). A skin biopsy specimen showed the marked proliferation of atypical tumor cells forming nests with adenoid structures. Immunohistochemical examination revealed that the tumor cells were negative for epithelial membrane antigen, carcinoembryonic antigen, and gross cystic disease fluid protein-15. Examination by positron emission tomography combined with computed tomography did not detect any lesions other than the axillary one, along with what were probably multiple metastatic lesions in the bones. It was obvious that the tumor in the axilla was located apart from the normal mammary gland. The patient had neither an apparent tumor in the breast nor a history of breast carcinoma. The tumor on the axilla was excised with a 2-cm horizontal margin, and left axillary lymph node dissection was performed. Histologic findings of the resected specimens showed invasive ductal carcinoma with cartilaginous metaplasia, consistent with accessory breast carcinoma (Fig 2).

Immunohistochemically, the resected tumor cells were negative for estrogen receptor and

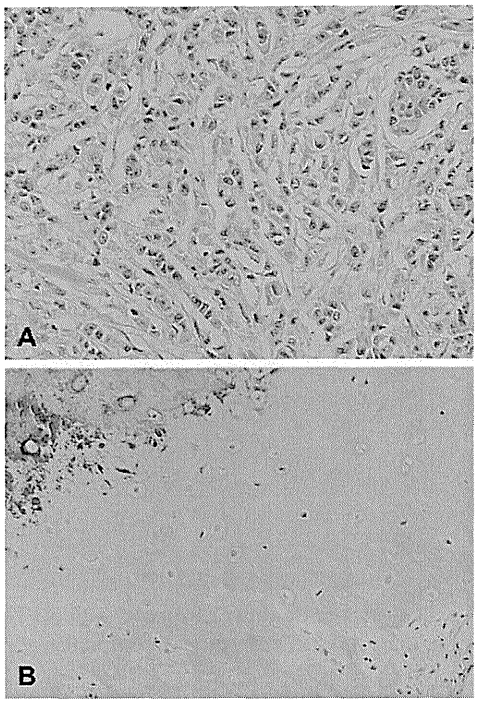

Fig 2. Carcinoma arising from accessory breast. Histologic features of resected tumor. **A,** Tumor cells in single file rows have large hyperchromatic atypical nuclei. **B,** In some parts of tumor, cartilaginous metaplasia is observed. (**A** and **B,** Hematoxylin-eosin stain; original magnifications: ×400.)

progesterone receptor, and positive for human epidermal growth factor receptor type 2. We diagnosed the case as metaplastic carcinoma arising from accessory breast. Metastasis was seen in 24 of 39 resected axillary lymph nodes. The patient was treated with trastuzumab. However, brain metastases developed and the patient died 6 months after the operation.

A thorough search of the English-language literature found only 1 case of accessory breast cancer in a man.[4]

Our patient already had multiple bone metastases when the diagnosis was established. Breast carcinoma in men generally has a poorer prognosis than in women, because the diagnosis tends to be delayed. In human epidermal growth factor receptor type 2–positive breast cancer, trastuzumab has been shown to be very effective, although it cannot cross the blood-brain barrier.[5] The current patient developed cerebellar metastases during treatment with trastuzumab.

This case suggests that we should keep accessory breast cancer in mind as a differential diagnosis for large subcutaneous tumors on the axillae, even though accessory breast cancer in men is extremely rare.

Yukari Yoshida, MD,[a] Akihiro Sakakibara, MD, PhD,[a] Tomohisa Watanabe, MD,[a] Kimitoshi Noto, MD,[b] Kenichi Sakita, MD, PhD,[c] Yu Sakai, MD, PhD,[c] Takeshi Amemiya, MD, PhD,[d] and Masashi Akiyama, MD, PhD[e]

Divisions of Dermatology,[a] Orthopedics,[b] Pathology,[c] and Surgery,[d] Anjo-Kosei Hospital, Anjo, Aichi; and Department of Dermatology, Nagoya University Graduate School of Medicine,[e] Nagoya, Japan

Funding sources: None.

Conflicts of interest: None declared.

Correspondence to: Masashi Akiyama, MD, PhD, Department of Dermatology, Nagoya University Graduate School of Medicine, 65 Tsurumai-cho, Showa-ku, Nagoya 466-8550, Japan

E-mail: makiyama@med.nagoya-u.ac.jp

REFERENCES

1. Kitamura K, Kuwano H, Kiyomatsu K, Ikejiri K, Sugimachi K, Saku M. Mastopathy of the accessory breast in the bilateral axillary regions occurring concurrently with advanced breast cancer. Breast Cancer Res Treat 1995;35:221-4.
2. Marshall MB, Moynihan JJ, Frost A, Evans SR. Ectopic breast cancer: case report and literature review. Surg Oncol 1994;3:295-304.
3. Azuma T, Yamamoto K, Kobayashi T, Nakano H. Accessory breast cancer: a case report of carcinoma originating from aberrant breast tissue in the axillar region. Breast Cancer 1997;4:49-52.
4. Takeyama H, Takahashi H, Tabei I, Fukuchi O, Nogi H, Kinoshita S, et al. Malignant neoplasm in the axilla of a male: suspected primary carcinoma of an accessory mammary gland. Breast Cancer 2010;17:151-4.
5. Bravo Marques JM. Treatment of brain metastases in patients with HER2+ breast cancer. Adv Ther 2009;26(Suppl):S18-26.

http://dx.doi.org/10.1016/j.jaad.2012.04.034

Pemphigus herpetiformis: Report of a rare case

To the Editor: A 42-year-old man presented with a 3-year history of extremely pruritic, erythematous, urticarial plaques, some with annular rings of tense vesicles at the periphery (Fig 1). The lesions were scattered on the trunk and proximal extremities, involving approximately 40% of the total body surface area. A lesional skin biopsy specimen initially demonstrated neutrophilic spongiosis with rare eosinophils (Fig 2). Deeper sections, however, showed suprabasilar acantholysis with scattered neutrophils (Fig 2, *inset*). A perilesional skin biopsy sent for direct immunofluorescence (DIF) revealed intercellular IgG and C3, most prominent in the lower layers of the epidermis. Antibodies to desmoglein 1, but not desmoglein 3, were demonstrated by enzyme-linked

Journal of Dermatological Science 67 (2012) 37–43

Contents lists available at SciVerse ScienceDirect

Journal of Dermatological Science

journal homepage: www.elsevier.com/jds

A group of atopic dermatitis without IgE elevation or barrier impairment shows a high Th1 frequency: Possible immunological state of the intrinsic type

Rieko Kabashima-Kubo [a], Motonobu Nakamura [a], Jun-ichi Sakabe [a,b], Kazunari Sugita [a], Ryosuke Hino [a], Tomoko Mori [a], Miwa Kobayashi [a], Toshinori Bito [a,c], Kenji Kabashima [a,d], Koetsu Ogasawara [e], Yukiko Nomura [f], Toshifumi Nomura [f], Masashi Akiyama [f,g], Hiroshi Shimizu [f], Yoshiki Tokura [a,b,*]

[a] Department of Dermatology, University of Occupational and Environmental Health, Kitakyushu, Japan
[b] Department of Dermatology, Hamamatsu University School of Medicine, Hamamatsu, Japan
[c] Department of Dermatology, Kobe University Graduate School of Medicine, Kobe, Japan
[d] Department of Dermatology, Faculty of Medicine, Kyoto University Graduate School of Medicine, Kyoto, Japan
[e] Department of Immunobiology, Institute of Development, Aging and Cancer, Tohoku University, Sendai, Japan
[f] Department of Dermatology, Hokkaido University Graduate School of Medicine, Sapporo, Japan
[g] Department of Dermatology, Nagoya University Graduate School of Medicine, Nagoya, Japan

ARTICLE INFO

Article history:
Received 29 November 2011
Received in revised form 15 March 2012
Accepted 10 April 2012

Keywords:
Atopic dermatitis
Extrinsic
Intrinsic
IgE
Filaggrin
Th1
Th2

SUMMARY

Background: Atopic dermatitis (AD) can be classified into the major extrinsic type with high serum IgE levels and impaired barrier, and the minor intrinsic type with normal IgE levels and unimpaired barrier.
Objective: To characterize the intrinsic type of Japanese AD patients in the T helper cell polarization in relation to the barrier condition.
Methods: Enrolled in this study were 21 AD patients with IgE < 200 kU/L (IgE-low group; 82.5 ± 59.6 kU/L) having unimpaired barrier, and 48 AD patients with IgE > 500 kU/L (IgE-high group; 8.050 ± 10.400 kU/L). We investigated filaggrin gene (*FLG*) mutations evaluated in the eight loci common to Japanese patients, circulating Th1, Th2 and Th17 cells by intracellular cytokine staining and flow cytometry, and blood levels of CCL17/TARC, IL-18, and substance P by ELISA.
Results: The incidence of *FLG* mutations was significantly lower in the IgE-low group (10.5%) than the IgE-high group (44.4%) (normal individuals, 3.7%). The percentage of IFN-γ-producing Th1, but not Th2 or Th17, was significantly higher in the IgE-low than IgE-high group. Accordingly, Th2-attracting chemokine CCL17/TARC, was significantly lower in the IgE-low than the IgE-high group. There were no differences between them in serum IL-18 levels, or the plasma substance P levels or its correlation with pruritus.
Conclusion: The IgE-low group differed from the IgE-high group in that it had much less *FLG* mutations, increased frequency of Th1 cells, and lower levels of CCL17. In the intrinsic type, non-protein antigens capable of penetrating the unimpaired barrier may induce a Th1 eczematous response.

1. Introduction

Despite a large number of clinical, laboratory and experimental studies, the pathophysiology of AD remains unfully elucidated, because AD has heterogeneous aspects. The clinical phenotype of AD can be classified into the extrinsic and intrinsic types [1,2]. Since there is still no sufficient consensus whether the intrinsic type is a distinct entity, some researchers denominate it atopiform dermatitis [3]. Nevertheless, the classification into the extrinsic and intrinsic AD has been widely used, as various kinds of clinical studies have been performed under this dichotomy in many countries, including Germany [1,4,5], Netherland [3], Hungary [6], Italy [7,8], Korea [9,10], and Japan [11].

Extrinsic and intrinsic AD are defined according to IgE-mediated sensitization, namely the presence or absence of specific IgE for environmental and food allergens [10–12]. Whereas the extrinsic patients have high levels of serum IgE, the intrinsic type shows normal IgE levels, no specific IgE, and negative skin-prick test to common aeroallergens or food allergens [13]. Since total serum IgE values are correlated with the allergen-specific IgE status [14,15], total IgE can be regarded as a clinically useful parameter to expectedly differentiate between the extrinsic and

* Corresponding author at: Department of Dermatology, Hamamatsu University School of Medicine, 1-20-1 Handayama, Higashi-ku, Hamamatsu 431-3192, Japan. Tel.: +81 53 435 2303; fax: +81 53 435 2368.
E-mail address: tokura@hama-med.ac.jp (Y. Tokura).

0923-1811/$36.00
http://dx.doi.org/10.1016/j.jdermsci.2012.04.004

Table 1
Patients enrolled in this study.

Number of subjects	IgE-high group	IgE-low group	
	46 (19 men and 27 women)	21 (7 men and 14 women)	
Age (years, mean ± SD)	30.5 ± 13.2	34.8 ± 13.4	$P = 0.226$
IgE (kU/L, mean ± SD)	8.050 ± 10.400	82.5 ± 59.6	$P < 0.001$
RAST for *D. pteronyssinus* (class, mean ± SD)	5.64 ± 0.693	1.77 ± 1.73	$P < 0.001$
LDH (IU/L, mean ± SD)	269 ± 91.2	206 ± 69.0	$P = 0.0129$
Eosinophils (%, mean ± SD)	8.79 ± 6.02	5.65 ± 5.45	$P = 0.0800$
VAS (mean ± SD)	54.2 ± 27.0	50.2 ± 23.0	$P = 0.686$
SCORAD (mean ± SD)	35.4 ± 16.1	31.3 ± 11.3	$P = 0.410$
TEWL ($g/m^2/h$, mean ± SD)	14.3 ± 7.57*	8.73 ± 3.74	$P = 0.0440$
Skin surface hydration (AU, mean ± SD)	29.2 ± 7.28*	34.7 ± 5.78	$P = 0.0250$

The normal ranges or values are as follows: LDH, 119–229 IU/L; TEWL, 6.58 ± 1.78 $g/m^2/h$; skin surface hydration (capacitance), 39.2 ± 14.4 AU.
* Statistically significant, compared to normal subjects.

intrinsic types in both adults [4,11] and children [14]. There are some differences in the frequency of intrinsic AD [15] among the countries, as reported as 27% [16], 37% [14], 12% [6], and 22% [11]. The female predominance has been consistently observed in intrinsic AD by a number of studies [1,3,15,17]. Females made up 76.5% of Intrinsic AD patients in our former study [11].

The original concept of "intrinsic" type represents the non-allergic nature, however, similarly to the extrinsic type, the intrinsic type may show eosinophilia. More fundamentally, both types represent eczematous dermatitis, a manifestation of the delayed-type or late-phase reaction. Therefore, the intrinsic type AD is not a non-allergic type, but is induced *via* some immunological mechanism.

When assessed by transepidermal water loss (TEWL), skin surface hydration, and perception threshold of electric stimuli, extrinsic AD patients showed an impaired barrier function, but intrinsic AD retained the normal barrier function and sensory reactivity to external pruritic stimuli [11]. The recent identification of loss-of-function mutations in filaggrin gene (*FLG*) sheds new light on the mechanisms of AD [18,19]. These mutations represent a strong predisposing factor for AD and asthma in various countries [20–23]. Perturbation of skin barrier function as a result of reduction or complete loss of filaggrin expression leads to enhanced percutaneous transfer of allergens. *FLG* mutations are associated seemingly with the extrinsic type of AD [20] and palmar hyperlinearity, which represents a shared feature of AD and ichthyosis vulgaris. Accordingly, palmar hyperlinearity is rarely observed in the intrinsic type [3]. Therefore, it is expected that intrinsic AD patients lack a mutation in *FLG*.

AD is well known as a Th2-polarized disease. However, some differences in systemic cytokine skewing have been reported between the extrinsic and intrinsic AD. Extrinsic AD shows high levels of Th2 cytokines, interleukin (IL)-4, IL-5 and IL-13, and intrinsic AD is linked with lower levels of IL-4 and IL-13 [7]. Along with the elevation of IL-5 [24], eosinophil counts [10] and eosinophil cationic protein levels [16] are increased in extrinsic AD. However, another report demonstrated that both extrinsic and intrinsic AD patients showed increased production of IL-5 and

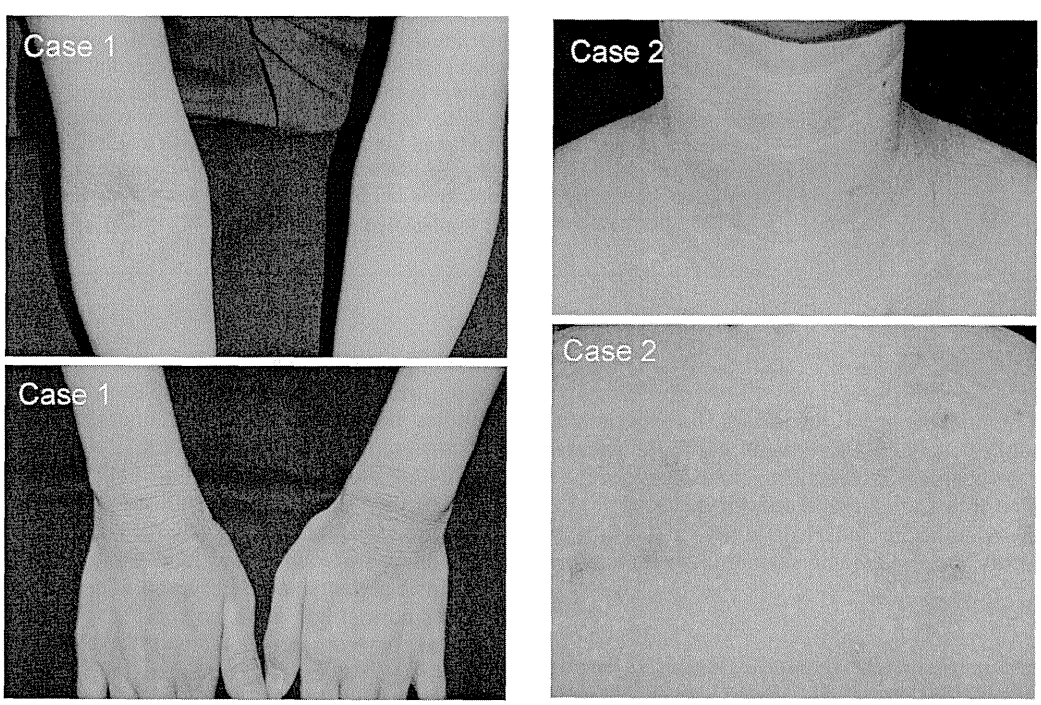

Fig. 1. Clinical photographs of the representative IgE-low AD patients. Case 1 (left): a 25-year-old female, with total serum IgE, 69 kU/L; and blood eosinophils, 10%. A lichenified eruption on the antecubital fossae (top, left) and the dorsal aspects of the wrists (bottom, left). She also had chronic eczema on the neck and trunk and was diagnosed as having AD in childhood. Case 2 (right): a 29-year-old female, with total serum IgE, 43 kU/l; and blood eosinophils, 11%. A lichenified eruption on the neck, upper chest (top, right), and back (bottom, right). The skin lesions had been diagnosed as AD since childhood.

IL-13 [25]. In addition, a more recent finding of the involvement of IL-17-producing Th (Th17) cells [26] raises an issue whether Th17 cells are more deeply associated with extrinsic or intrinsic AD.

These several different lines of evidence suggest the relationship between the skin barrier condition and helper T cell polarization in AD. We sought to investigate the immunological state of AD patients without elevation of serum IgE or impairment of barrier function. We first examined whether those patients had *FLG* mutations, and then investigated the frequencies of circulating Th1, Th2 and Th17 subsets with CCL17/TARC Th2 chemokine measurement. Results imply that the intrinsic AD is an immunological disorder fundamentally different from extrinsic AD.

2. Materials and methods

2.1. Participants and background assessments

Sixty-seven patients with AD (aged 9–59 years; 26 men and 41 women), and 10 healthy non-AD volunteers with low serum IgE levels (aged 28–38 years; 5 men and 5 women) were enrolled in this study. AD was diagnosed according to the criteria of Hanifin and Rajka classification [27]. The reported range or mean value of total serum IgE in the intrinsic type are from 22.2 to 134 kU/L, or alternatively, IgE values less than 150 or 200 kU/L have been used for an indication of intrinsic AD [15]. Our study of Japanese patients also showed that the mean value of total seurm IgE was 110.5 kU/mL (11–219 kU/L) [11]. In this study, we first selected 21 AD patients with IgE < 200 kU/L (mean ± SD, 82.5 ± 59.6 kU/L). As the control counterpart, 46 AD patients with IgE > 500 kU/L (8.050 ± 10.400 kU/L) were then selected. They were designated as the IgE-low and IgE-high groups, respectively. The disease activity was assessed by severity scoring of AD (SCORAD), and current itching was rated on a 100-mm visual analogue scale (VAS). The barrier function of stratum corneum was assessed by the skin surface hydration and TEWL [11]. The details of the patients were listed in Table 1. This study was conducted according to the Declaration of Helsinki Principles, performed after obtaining an informed consent from the patients, and approved by the Medical Ethical Committees of University of Occupational and Environmental Health and the Medical Ethical Committee of Hokkaido University Graduate School of Medicine.

2.2. FLG genotyping

FLG mutation analysis was performed in 18 patients of the IgE-high group (9 men and 9 women) and 19 patients of the IgE-low group (7 man and 12 women). All genomic DNA samples from the patients were screened for the eight previously reported Japanese-specific *FLG* mutations (R501X, 3321delA, S1695X, Q1701X, S2554X, S2889X, S3296X and K4022X) as described previously [21,28].

2.3. Intracellular cytokine staining and flow cytometric analysis of peripheral blood mononuclear cells (PBMCs)

Peripheral blood mononuclear cells (PBMCs) were isolated by standard Ficoll-Paque method. Intracellular cytokines were stained according to the protocol of Cytostain (Immunotech, Marseille, France) (26). Briefly, cells (2×10^6 cells/mL) were stained with PerCP-conjugated anti-CD8 monoclonal antibody (mAb), APC-conjugated anti-CD3 mAb (BD Biosciences), phycoerythrin-labeled anti-IL-17, IL-4, or IL-5, and FITC-labeled anti-IFN-γ mAb (all from BD Biosciences). Fluorescence profiles were analyzed by flow cytometry in FACSCanto (BD Biosciences). The percentage of $CD3^+$ $CD8^-$ cells bearing each cytokine was counted.

2.4. Naïve B cell isolation from PBMCs and quantitation of IgE in culture supernatants

Naïve B cells were separated from PBMCs of IgE-high AD patients using Naïve B Cell isolation Kit II (Miltenyi Biotec, Gladbach, Germany) and autoMACS (Miltenyi Biotec). 1×10^5 purified naïve B cells were cultured in RPMI-1640 in the presence of recombinant human IL-4 (10 μg/mL; R&D systems, Minneapolis, MN) and recombinant human CD40L (CD154) (200 μg/mL; R&D systems) for 2 weeks in the presence of 1, 5, 20 ng/mL of IFN-γ (R&D Systems, Inc). Culture supernatants were collected after 2 weeks, and IgE content was measured using Human IgE ELISA Quantitation Kit (Bethyl, Montgomery, TX).

2.5. CCL17/TARC and IL-18 measurements in sera

Serum CCL17/TARC and IL-18 levels were measured by ELISA (Special Reference Laboratories, Tokyo, Japan) in 20 AD patients with the IgE-high group (9 men and 11 women), 19 AD patients with the IgE-low group (6 men and 13 women) and 9 normal subjects (3 men and 6 women).

2.6. Substance P (SP) measurement

The concentration of plasma SP was measured by Kyowa Medex Co in 18 IgE-high AD patients (7 men and 11 women) and 12 IgE-low AD patients (4 men and 8 women).

Table 2
FLG mutations in IgE-high and IgE-low AD groups.

Case	Age	Sex	IgE(kU/L)	*FLG* mutation
IgE-high				
1	21	M	19,000	S2889X
2	19	M	2800	WT
3	24	M	675	3321delA, S2889X
4	25	F	22,000	S3296X
5	36	F	3790	WT
6	49	F	885	WT
7	29	F	53,000	WT
8	40	M	2120	3321delA, Q1701X
9	32	F	19,000	WT
10	45	M	10,000	WT
11	15	F	1600	3321delA
12	21	F	5200	WT
13	36	M	1060	WT
14	19	M	1360	S2889X
15	15	F	1090	WT
16	31	M	53,000	3321delA
17	30	F	567	WT
18	22	M	1320	WT
IgE-low				
1	28	F	43	WT
2	21	F	20	WT
3	25	F	69	WT
4	32	F	187	WT
5	59	M	81	WT
6	20	M	186	WT
7	32	F	67	K4022X
8	49	F	80	WT
9	18	F	45	WT
10	30	M	87	WT
11	37	M	6	WT
12	32	M	109	WT
13	22	F	14	WT
14	30	F	36	WT
15	46	F	44	Q1701X
16	27	F	14	WT
17	24	F	24	WT
18	43	M	148	WT
19	30	M	167	WT

WT: wild type.

2.7. Statistical analysis

Student's *t*-test (unpaired) and Fisher's test were employed to determine statistical differences. For all tests, *P*-value < 0.05 was considered statistically significant.

3. Results

3.1. Background of patients

Enrolled in this study were AD patients with he IgE-high (>500 kU/L) and IgE-low (<200 kU/L) groups with the mean values of 8.050 and 82.5 kU/L, respectively (Table 1). We first selected AD patients belonging to the IgE-low group, and their skin manifestations (Fig. 1) were indistinguishable from the IgE-high patients. IgE RAST was scored by index values 0–6 according to the manufacturer's criteria (BML, Tokyo, Japan): class 0 (≤0.34 UA/mL), class 1 (0.35–0.69 UA/mL), class 2 (0.70–3.49 UA/mL), class 3 (3.50–17.4 UA/mL), class 4 (17.5–49.9 UA/mL), class 5 (50.0–99.9 UA/mL), and class 6 (≥100 UA/mL). As a representative aeroallergen, we chose *Dermatophagoides pteronyssinus*. An index value ≥4 to *D. pteronyssinus* was obtained in 100% (18/18) of the IgE-high patients examined. Moreover, 75% of the IgE-high AD patients showed RAST score index value of 6, and none of the IgE-low patients showed this highest score. When expressed by the mean ± SD, the IgE-high group had score levels as high as class 5.64, whereas the low group had class 1.77. The RAST score for *Dermatophagoides farinae* showed virtually the same data. No significant difference was noted in age between the two groups. Women predominated in the IgE-low patients, as already noted [1,3,15,17]. SCORAD and VAS tended to be higher in the IgE-high than the IgE-low group, as reported previously in intrinsic AD [4,6,29]. Skin surface hydration was significantly lower in the IgE-high than the IgE-low AD and healthy controls, and TEWL, another assessment of the barrier function, was significantly higher in the IgE-high than the IgE-low AD and normal controls [11]. Thus, the skin barrier function was preserved in the IgE-low AD.

3.2. Significantly low incidence of FLG mutations in IgE-low group

We investigated *FLG* mutations in 18 IgE-high and 19 IgE-low AD patients with the previously reported method for Japanese AD patients [21]. Only 2 IgE-low cases (10.5%) had mutations in *FLG*, whereas 8 of 18 IgE-high patients (44.4%) possessed *FLG* mutations (Table 2). There was statistical significance between the two groups in the mutation incidence ($P = 0.0246$), suggesting that *FLG* mutations are less prevalent in the IgE-low group. The frequency of *FLG* mutations among normal controls without any history of allergy is 3.7%. In the IgE-high patients, there was no statistical difference in SCORAD or IgE level between the *FLG* mutation-bearing and *FLG* mutation-lacking patients.

3.3. Higher circulating Th1 cell frequency in the IgE-low group

The percentages of Th1, Th2 and Th17 cells in PBMCs were examined by flow cytometry after intracellular staining for IFN-γ,

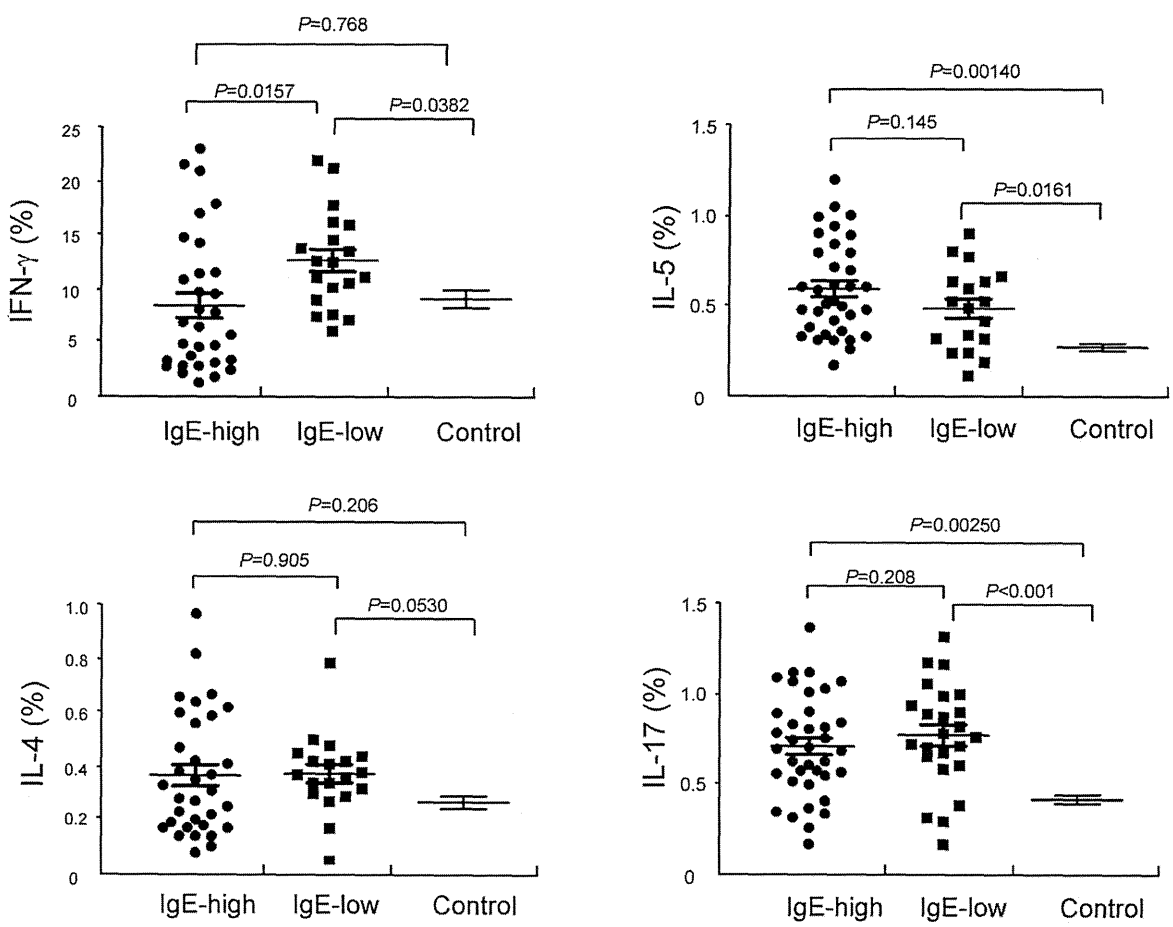

Fig. 2. Percentages of IFN-γ, IL-4, IL-5, and IL-17-positive $CD4^+$ cells. PBMCs from patients were incubated with PMA and Ca ionophore. They were then stained for CD3 and CD8, and subsequently stained intracellularly for IFN-γ, IL-4, IL-5, and IL-17. Since the stimulation with PMA and Ca ionophore downregulates the expression of CD4, $CD4^+$ cells positive for each cytokine was expressed as follows: (% $CD3^+$ cells positive for each cytokine) – (% $CD8^+$ cells positive for each cyokine). The vertical bars and error bars represent the mean ± SD.

IL-4, IL-5, and IL-17. The most intriguing finding is that the percentage of IFN-γ$^+$ T cells was significantly higher in the IgE-low than IgE-high group (Fig. 2). There was no significant difference in the IL-4, IL-5 or IL-17-positive cell frequency between the two types. These three cytokine-positive cells were increased in both groups of AD compared to the control.

3.4. Downregulation of B cell IgE production by IFN-γ

The above finding indicates that the IgE-low AD patients have high frequencies of IFN-γ$^+$ Th1 cells as well as low levels of IgE. To address the mechanism of this correlation, naïve B cells were purified from PBMCs of two patients with the IgE-high AD patients. The addition of IL-4 and CD40L (CD154) promoted class-switching and IgE production by B cells, which was inhibited by the addition of IFN-γ as low as 1 ng/mL (Fig. 3). This provides an implication that IFN-γ contributes to the normal level of IgE in the IgE-low AD.

3.5. Blood levels of CCL17/TARC, IL-18, and SP in the IgE-high and IgE-low AD groups

CCL17/TARC is a Th2 cell-attracting chemokine and its serum level is associated with the disease activity of AD [30]. IL-18 is possibly involved in the pathogenesis of AD [31], especially in the intrinsic type through the induction of IFN-γ. We therefore investigated serum CCL17/TARC and IL-18 levels in 20 IgE-high and 19 IgE-low patients. Both groups had higher levels of serum CCL17 than healthy control. Notably, its value was significantly higher in the IgE-high than the IgE-low group (Fig. 4). There was no significant difference in serum IL-18 level between the two groups of AD, as the means ± SD of IL-18 were 104.4 ± 34.97 (n = 20) in the IgE-high group and 92.40 ± 44.83 (n = 19) in the IgE-low group.

Given the original idea that external allergens are not causative in the intrinsic type, neurogenic inflammation induced by neuropeptides might be more important in this type of AD [32]. To address this issue, we measured plasma levels of SP in the two groups. The levels of SP in the IgE-high and IgE-low groups were comparable, as they were 50.6 ± 20.6 pg/mL and 59.5 ± 23.0 pg/mL, respectively. In both groups, SP levels and VAS for pruritus significantly correlated with each other (Fig. 5), indicating no dominancy of neuropeptides for the IgE-low group.

4. Discussion

The IgE-low type is a minor population of AD, but its pathophysiology is an issue of interest. In this study, we compared the IgE-low AD patients with the IgE-high patients, focusing on *FLG* mutations and the systemic Th1/Th2 polarization. The IgE-low group retained the common AD properties, *i.e.* typical clinical manifestations, eosinophilia, and increased circulating Th2 cell percentage. However, it showed a normal barrier function with a lower frequency of *FLG* mutations and an increased number of IFN-γ-producing Th1 cells. In accordance with our data, it has been reported that *FLG* mutations predispose to early-onset and extrinsic AD [20].

Regarding Th1/Th2 polarization, it has been reported that extrinsic AD shows high levels of Th2 cytokines and intrinsic AD is linked with lower levels of them [7]. The apoptosis of circulating memory/effector Th1 cells is confined to extrinsic AD patients, whereas intrinsic AD patients show no evidence for enhanced T cell apoptosis *in vivo* [33]. Another group of investigators demonstrated that both extrinsic and intrinsic AD patients had increased production of IL-5 and IL-13 [25], but when PBMCs were stimulated with anti-CD3 antibody, extrinsic AD patients had a decreased capacity to produce IFN-γ [25]. Accordingly, IFN-γ$^+$ T cell frequency was higher in the IgE-low than IgE-high group in our

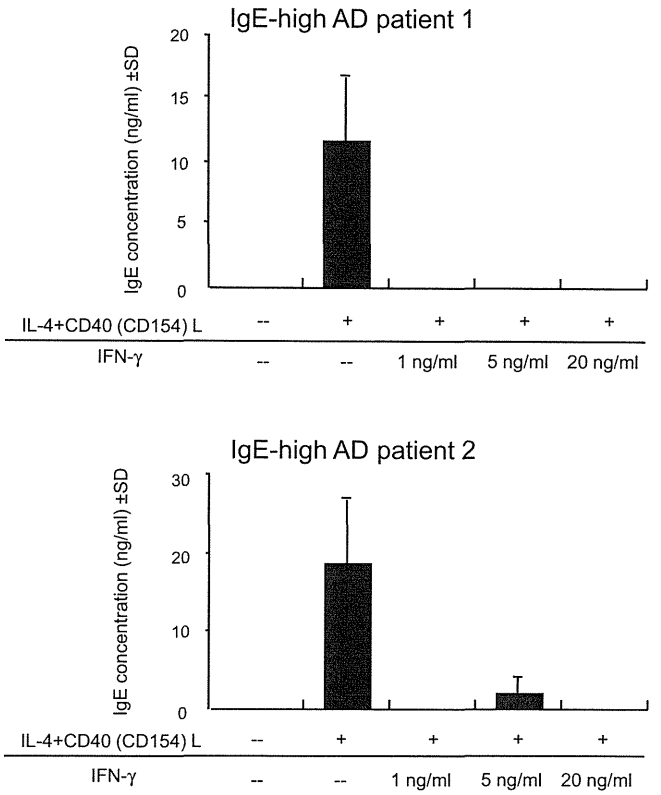

Fig. 3. IFN-γ-downregulation of IgE production by B cells from IgE-high AD patients. PBMCs from 2 patients with IgE-high AD were purified for naïve B cells. They were stimulated with IL-4 and CD40L (CD154) to produce IgE. IFN-γ was simultaneously added to the culture at a concentration of 1, 5, or 20 ng/mL.

study. Although no significant difference was found in the percentages of IL-4$^+$, IL-5$^+$ or IL-17$^+$ T cells, Th2 cells tended to be higher in the IgE-high group. Thus, intrinsic AD may have a less Th2-skewing state and rather shows a high expression level of IFN-γ. The elevation of serum CCL17/TARC, a Th2 attractive chemokine, in the IgE-high AD further supported this notion. In the skin lesions, eosinophils infiltrate more markedly in the extrinsic than intrinsic type [9,34], suggesting the less Th2 and more Th1 preponderant state in the skin as well. The overproduction of IFN-γ may further downregulate IgE production in the IgE-low AD, as suggested by our *in vitro* study.

A non-IgE-associated, mouse AD model may be regarded as a mimicry of human intrinsic AD [35]. In this model, IL-18 contributes to the spontaneous development of skin lesions

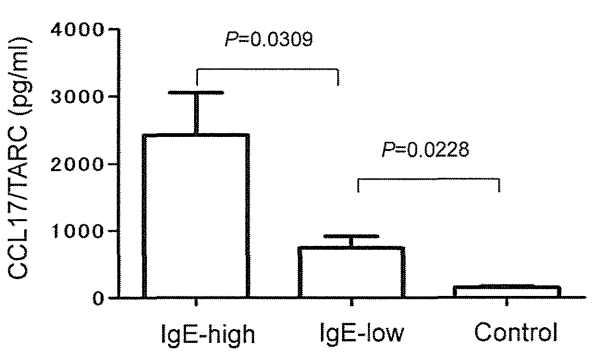

Fig. 4. Blood CCL17/TARC in IgE-high and IgE-low AD. Serum samples were obtained from IgE-high AD patients (n = 20), IgE-low AD patients (n = 19) and control subjects (n = 9). The means ± SD were 2430 ± 2820 in IgE-high AD and 851 ± 771 in IgE-low AD.

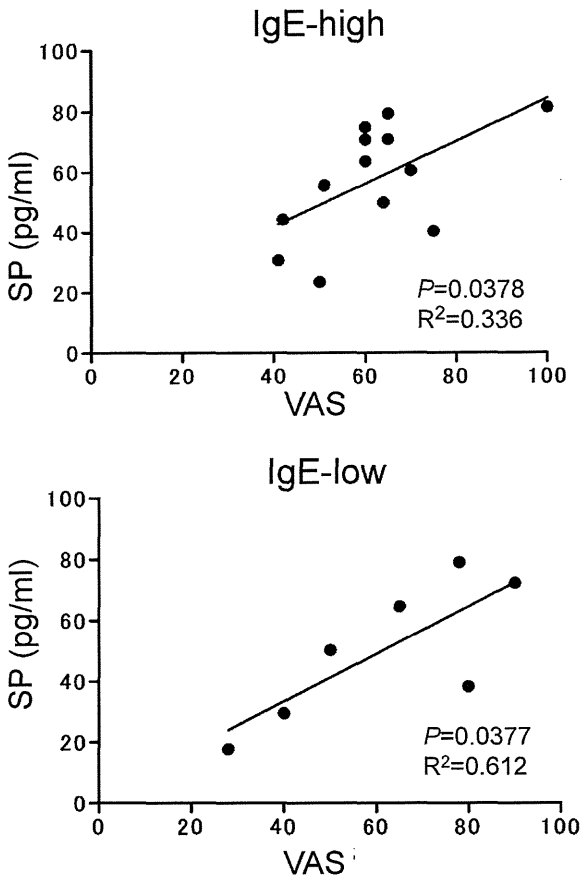

Fig. 5. Blood SP levels in IgE-high and IgE-low AD. Plasma SP levels were measured as described in Section 2, and simultaneously, VAS for pruritus was measured in the individual patients.

independently of IgE [36]. The mice can develop AD lesions with dermal infiltration of eosinophils and mast cells and showed an increase in serum levels of IL-18, but not IgE. This mouse model resembles intrinsic AD, since IFN-γ is an IL-18-promoted cytokine. However, we could not find a significant elevation of serum IL-18 in our IgE-low AD patients compared to the IgE-high patients. Thus, the IL-18 mediation remains unclear in human intrinsic AD.

In a mouse model of contact hypersensitivity, the responses to hapten are increased when a hapten is applied to the barrier-damaged skin [37]. Not only increased skin permeability but also altered immune functions of epidermal cells potentiate T-cell activation in acute barrier disruption [37]. The mRNA expression levels of Th2 chemokines and eosinophil chemoattractant are high in the epidermal cells from barrier-disrupted Th2-skewing BALB/c mice [38]. Th1 and Th2 chemokines are derived mainly from keratinocytes and Langerhans cells, respectively, and one of the crucial actions of IFN-γ is upregulation of keratinocyte production of Th1 chemokines and downregulation of Langerhans cell production of Th2 chemokines [39]. Therefore, the barrier damage likely induces infiltrates of Th2 cells and eosinophils in extrinsic AD, but their infiltrates are inhibited by IFN-γ in intrinsic AD.

We also examined SP levels in the IgE-high and IgE-low AD patients. It has been reported that neurotrophins, such as nerve growth factor (NGF) and brain-derived neurotrophic factor (BDNF), are increased in both extrinsic and intrinsic AD, suggesting the presence of a similar pathophysiologic background implicating a neuroimmune network [40]. However, there is a significant correlation between BDNF and SCORAD in the intrinsic but not extrinsic type [40]. Maternal NGF levels were high in both extrinsic and intrinsic AD [29]. We found that there was no difference in SP levels between the two groups, and these SP levels were correlated with the itch levels in both groups. This may imply that neurogenic inflammation is not a characteristic feature of intrinsic AD.

The normal barrier function and IFN-γ-producing potency of the IgE-low AD suggest that the patients are not sensitized with protein allergens, which are known to induce Th2 responses, but with other non-protein antigens. It is assumed that protein antigens are not allowed to enter into the skin in intrinsic AD because of the normal barrier. Instead, non-protein antigens, such as metals and haptens, can penetrate through the barrier and may induce Th1 as well as Th2 responses. In 137 atopic children, 19.3% patients were positive to metals [41], although the two types of AD were not separately studied. In 1965, Shanon reported that patients with metal allergy occasionally exhibit a skin manifestation indistinguishable from AD under the name of "pseudo-atopic dermatitis" [42]. Further investigation on this issue might clarify the pathophysiology of intrinsic AD.

Funding sources

None.

Acknowledgments

This work is supported by Grants-in Aid for Science Research from the Ministry of Health, Labour, and Welfare of Japan; and the Ministry of Education, Science, Sports, and Culture of Japan. We thank Ms. Rie Murase, Ms. Yukako Miyazaki, and Ms. Tamae Oishi for their technical assistance.

References

[1] Novak N, Bieber T. Allergic and nonallergic forms of atopic diseases. J Allergy Clin Immunol 2003;112:252–62.
[2] Tokura Y. Extrinsic and intrinsic types of atopic dermatitis. J Dermatol Sci 2010;58:1–7.
[3] Brenninkmeijer EE, Spuls PI, Legierse CM, Lindeboom R, Smitt JH, Bos JD. Clinical differences between atopic and atopiform dermatitis. J Am Acad Dermatol 2008;58:407–14.
[4] Folster-Holst R, Pape M, Buss YL, Christophers E, Weichenthal M. Low prevalence of the intrinsic form of atopic dermatitis among adult patients. Allergy 2006;61:629–32.
[5] Schafer T, Kramer U, Vieluf D, Abeck D, Behrendt H, Ring J. The excess of atopic eczema in East Germany is related to the intrinsic type. Br J Dermatol 2000;143:992–8.
[6] Ponyai G, Hidvegi B, Nemeth I, Sas A, Temesvari E, Karpati S. Contact and aeroallergens in adulthood atopic dermatitis. J Eur Acad Dermatol Venereol 2008;22:1346–55.
[7] Miraglia del Giudice M, Decimo F, Leonardi S, Maioello N, Amelio R, Capasso A, et al. Immune dysregulation in atopic dermatitis. Allergy Asthma Proc 2006;27:451–5.
[8] Ingordo V, D'Andria G, D'Andria C, Tortora A. Results of atopy patch tests with house dust mites in adults with 'intrinsic' and 'extrinsic' atopic dermatitis. J Eur Acad Dermatol Venereol 2002;16:450–4.
[9] Rho NK, Kim WS, Lee DY, Lee JH, Lee ES, Yang JM. Immunophenotyping of inflammatory cells in lesional skin of the extrinsic and intrinsic types of atopic dermatitis. Br J Dermatol 2004;151:119–25.
[10] Park JH, Choi YL, Namkung JH, Kim WS, Lee JH, Park HJ, et al. Characteristics of extrinsic vs. intrinsic atopic dermatitis in infancy: correlations with laboratory variables. Br J Dermatol 2006;155:778–83.
[11] Mori T, Ishida K, Mukumoto S, Yamada Y, Imokawa G, Kabashima K, et al. Comparison of skin barrier function and sensory nerve electric current perception threshold between IgE-high extrinsic and IgE-normal intrinsic types of atopic dermatitis. Br J Dermatol 2009;162:83–90.
[12] Wollenberg A, Kraft S, Oppel T, Bieber T. Atopic dermatitis: pathogenetic mechanisms. Clin Exp Dermatol 2000;25:530–4.
[13] Wuthrich B, Schmid-Grendelmeier P. The atopic eczema/dermatitis syndrome. Epidemiology, natural course, and immunology of the IgE-associated ("extrinsic") and the nonallergic ("intrinsic") AEDS. J Investig Allergol Clin Immunol 2003;13:1–5.
[14] Ott H, Stanzel S, Ocklenburg C, Merk HF, Baron JM, Lehmann S. Total serum IgE as a parameter to differentiate between intrinsic and extrinsic atopic dermatitis in children. Acta Derm Venereol 2009;89:257–61.
[15] Schmid-Grendelmeier P, Simon D, Simon HU, Akdis CA, Wuthrich B. Epidemiology, clinical features, and immunology of the "intrinsic" (non-IgE-mediated) type of atopic dermatitis (constitutional dermatitis). Allergy 2001;56:841–9.

[16] Ott H, Wilke J, Baron JM, Hoger PH, Folster-Holst R. Soluble immune receptor serum levels are associated with age, but not with clinical phenotype or disease severity in childhood atopic dermatitis. J Eur Acad Dermatol Venereol 2010;24:395–402.
[17] Novak N, Kruse S, Kraft S, Geiger E, Kluken H, Fimmers R, et al. Dichotomic nature of atopic dermatitis reflected by combined analysis of monocyte immunophenotyping and single nucleotide polymorphisms of the interleukin-4/interleukin-13 receptor gene: the dichotomy of extrinsic and intrinsic atopic dermatitis. J Invest Dermatol 2002;119:870–5.
[18] Smith FJ, Irvine AD, Terron-Kwiatkowski A, Sandilands A, Campbell LE, Zhao Y, et al. Loss-of-function mutations in the gene encoding filaggrin cause ichthyosis vulgaris. Nat Genet 2006;38:337–42.
[19] Palmer CN, Irvine AD, Terron-Kwiatkowski A, Zhao Y, Liao H, Lee SP, et al. Common loss-of-function variants of the epidermal barrier protein filaggrin are a major predisposing factor for atopic dermatitis. Nat Genet 2006;38:441–6.
[20] Weidinger S, Rodríguez E, Stahl C, Wagenpfeil S, Klopp N, Illig T, et al. Filaggrin mutations strongly predispose to early-onset and extrinsic atopic dermatitis. J Invest Dermatol 2007;127:724–6.
[21] Nomura T, Akiyama M, Sandilands A, Nemoto-Hasebe I, Sakai K, Nagasaki A, et al. Specific filaggrin mutations cause ichthyosis vulgaris and are significantly associated with atopic dermatitis in Japan. J Invest Dermatol 2008;128:1436–41.
[22] Novak N, Baurecht H, Schäfer T, Rodriguez E, Wagenpfeil S, Klopp N, et al. Loss-of-function mutations in the Filaggrin gene and allergic contact sensitization to nickel. J Invest Dermatol 2008;128:1430–5.
[23] Weidinger S, Illig T, Baurecht H, Irvine AD, Rodriguez E, Diaz-Lacava A, et al. Loss-of-function variations within the filaggrin gene predispose for atopic dermatitis with allergic sensitizations. J Allergy Clin Immunol 2006;118:214–9.
[24] Namkung JH, Lee JE, Kim E, Cho HJ, Kim S, Shin ES, et al. IL-5 and IL-5 receptor alpha polymorphisms are associated with atopic dermatitis in Koreans. Allergy 2007;62:934–42.
[25] Simon D, Von Gunten S, Borelli S, Braathen LR, Simon HU. The interleukin-13 production by peripheral blood T cells from atopic dermatitis patients does not require CD2 costimulation. Int Arch Allergy Immunol 2003;132:148–55.
[26] Koga C, Kabashima K, Shiraishi N, Kobayashi M, Tokura Y. Possible pathogenic role of Th17 cells for atopic dermatitis. J Invest Dermatol 2008;128:2625–30.
[27] Hanifin JM, Rajka G. Diagnostic features of atopic eczema. Acta Dermatol 1980;92:44–7.
[28] Nemoto-Hasebe I, Akiyama M, Nomura T, Sandilands A, McLean WHI, Shimizu H. FLG mutation p.Lys4021X in the C-terminal imperfect filaggrin repeat in Japanese patients with atopic eczema. Br J Dermatol 2009;161:1387–90.
[29] Wang IJ, Hsieh WS, Guo YL, Jee SH, Hsieh CJ, Hwang YH, et al. Neuro-mediators as predictors of paediatric atopic dermatitis. Clin Exp Allergy 2008;38:1302–8.
[30] Kakinuma T, Nakamura K, Wakuguma M, Mitsui H, Tada Y, Saeki H, et al. Thymus and activation-regulated chemokine in atopic dermatitis: serum thymus and activation-regulated chemokine level is closely related with disease activity. J Allergy Clin Immunol 2001;107:535–41.
[31] Shaker OG, El-Komy M, Tawfic SO, Zeidan N, Tomairek RH. Possible role of nerve growth factor and interleukin-18 in pathogenesis of eczematous lesions of atopic dermatitis. J Dermatol Sci 2009;53:153–4.
[32] Pavlovic S, Liezmann C, Blois SM, Joachim R, Kruse J, Romani N, et al. Substance P is a key mediator of stress-induced protection from allergic sensitization via modified antigen presentation. J Immunol 2011;186:848–55.
[33] Akdis M, Trautmann A, Klunker S, Daigle I, Kucuksezer UC, Deglmann W, et al. T helper (Th) 2 predominance in atopic diseases is due to preferential apoptosis of circulating memory/effector Th1 cells. FASEB J 2003;17:1026–35.
[34] Jeong CW, Ahn KS, Rho NK, Park YD, Lee DY, Lee JH, et al. Differential in vivo cytokine mRNA expression in lesional skin of intrinsic vs. extrinsic atopic dermatitis patients using semiquantitative RT-PCR. Clin Exp Allergy 2003;33:1717–24.
[35] Konishi H, Tsutsui H, Murakami T, Yumikura-Futatsugi S, Yamanaka K, Tanaka M, et al. IL-18 contributes to the spontaneous development of atopic dermatitis-like inflammatory skin lesion independently of IgE/stat6 under specific pathogen-free conditions. Proc Natl Acad Sci U S A 2002;99:11340–45.
[36] Terada M, Tsutsui H, Imai Y, Yasuda K, Mizutani H, Yamanishi K, et al. Contribution of IL-18 to atopic-dermatitis-like skin inflammation induced by Staphylococcus aureus product in mice. Proc Natl Acad Sci U S A 2006;103:8816–21.
[37] Nishijima T, Tokura Y, Imokawa G, Seo N, Furukawa F, Takigawa M. Altered permeability and disordered cutaneous immunoregulatory function in mice with acute barrier disruption. J Invest Dermatol 1997;109:175–82.
[38] Onoue A, Kabashima K, Kobayashi M, Mori T, Tokura Y. Induction of eosinophil- and Th2-attracting epidermal chemokines and cutaneous late-phase reaction in tape-stripped skin. Exp Dermatol 2009;18:1036–43.
[39] Mori T, Kabashima K, Yoshiki R, Sugita K, Shiraishi N, Onoue A, et al. Cutaneous hypersensitivities to hapten are controlled by IFN-g-upregulated keratinocyte Th1 chemokines and IFN-γ-downregulated langerhans cell Th2 chemokines. J Invest Dermatol 2008;128:1719–27.
[40] Raap U, Werfel T, Goltz C, Deneka N, Langer K, Bruder M, et al. Circulating levels of brain-derived neurotrophic factor correlate with disease severity in the intrinsic type of atopic dermatitis. Allergy 2006;61:1416–8.
[41] Giordano-Labadie F, Rance F, Pellegrin F, Bazex J, Dutau G, Schwarze HP. Frequency of contact allergy in children with atopic dermatitis: results of a prospective study of 137 cases. Contact Dermat 1999;40:192–5.
[42] Shanon J. Pseudo-atopic dermatitis. Contact dermatitis due to chrome sensitivity simulating atopic dermatitis. Dermatologica 1965;131:176–90.

Severe Chilblain Lupus Is Associated with Heterozygous Missense Mutations of Catalytic Amino Acids or their Adjacent Mutations in the Exonuclease Domains of 3′-Repair Exonuclease 1

Journal of Investigative Dermatology (2012) **132,** 2855–2857; doi:10.1038/jid.2012.210; published online 21 June 2012

TO THE EDITOR

Chilblain lupus (CL) is a subtype of chronic cutaneous lupus erythematosus. Familial CL (FCL), inherited via an autosomal dominant trait, has been described in two families segregating distinct mutations in the 3′-repair DNA exonuclease 1 (TREX1) (Lee-Kirsch *et al.*, 2007a; Rice *et al.*, 2007).

TREX1 is a potent 3′–5′ exonuclease that degrades single- and double-stranded DNA (ssDNA and dsDNA) in mammalian cells. TREX1 belongs to the exonuclease DEDDh family, whose members display low levels of sequence homology while possessing a common fold and identical active site organization termed the "DEDDh motif"(Brucet *et al.*, 2007).

Here we describe a Japanese case of FCL with the novel missense mutation p.Pro132Ala in *TREX1*. We demonstrate that the mutant TREX1 shows slightly reduced ssDNA cleavage function by *in vitro* exonuclease assays using recombinant mutant TREX1 proteins. A review of clinical features in patients with heterozygous missense mutations that are catalytic residues of or adjacent to the DEDDh motif in the three exonuclease domains of TREX1, including our case, revealed that all the patients had severe CL.

The patient was a 62-year-old Japanese woman with painful bluish-red infiltrates with atrophic branching and ulcers on the fingers, hands, toes, cheeks, lips, and nose, which persisted in all seasons (Figure 1a and b). The eruptions occurred from 1 year of age. Five of her relatives from three generations had similar skin symptoms from early childhood (Figure 1d). Apart from the skin findings, physical examination was unremarkable. She never had any neurological symptoms. Histological examination of lesional skin from the left hand showed typical features of lupus erythematosus (Figure 1c). Laboratory investigations revealed the presence of antinuclear antibodies showing a homogeneous pattern with a titer of 1:80. Circulating autoantibodies against dsDNA and ssDNA were undetectable. Serum IgA and IgG were slightly elevated. There was no serological evidence for viral or bacterial infections. All other laboratory values, including complete blood cell count with differential coagulation, circulating complement factors, and liver function tests, as well as urine analysis, were within normal ranges. On the basis of the clinical, serological, and histological findings, as well as family history, FCL was suspected.

The ethics committee of Nagoya University approved the studies described below. The study was conducted according to the Declaration of Helsinki Principles. The participants gave written informed consent. The coding region of *TREX1* was amplified from genomic DNA from blood by PCR. Direct sequencing of the patient's PCR products revealed that the patient carried the heterozygous missense mutation p.Pro132Ala (c.394 C>G) in *TREX1* (Figure 1e), which was not detected in the 100 control individuals (data not shown). The proline residue mutated by p.Pro132Ala is adjacent to the second aspartic acid residue of the DEDDh motif, an active catalytic site in the exonuclease domain of TREX 1 (Figure 2a). This proline residue was confirmed to be highly conserved in mammalians (Figure 2b). Thereafter, the ssDNA exonuclease activities were measured. Compared with the exonuclease activities of wild-type TREX1, those of TREX1 (P132A) were slightly reduced (Supplemental Figure S1 online).

TREX1 mutations are known to underlie four genetic disorders with distinctive phenotypes: Aicardi–Goutières syndrome (AGS), retinal vasculopathy with cerebral leukodystrophy, systemic lupus erythmatosus (SLE), and FCL (Crow *et al.*, 2006; Lee-Kirsch *et al.*, 2007b; Richards *et al.*, 2007). The majority of *TREX1* mutations causing autosomal recessive AGS are predicted to be complete loss-of-function mutations. Only three AGS cases caused by heterozygous *TREX1* mutations have been reported, and the causative *TREX1* mutations were p.Asp18Asn, p.Asp200Asn, and p.Asp200His. It is noteworthy that all three patients had early-onset CL (Rice *et al.*, 2007; Haaxma *et al.*, 2010; Ramantani *et al.*, 2010).

The mutations in *TREX1* in SLE patients were not reported in the exonuclease domains, except for the p.Arg128Asp mutation found in an SLE patient. The patient was suffering from neuropsychiatric lupus with digital gangrene (de Vries *et al.*, 2010).

With regard to FCL, only two *TREX1* mutations in two families have been reported. Rice *et al.* (2007) reported the *TREX1* mutation c.375dupT in an FCL family with 67% (2 of 3) symptomatic penetrance. The mutation produced p.Asp125fs, which causes defects in key catalytic domains in the

Abbreviations: AGS, Aicardi-Goutières syndrome; CL, chilblain lupus; dsDNA, double-stranded DNA; FCL, familial chilblain lupus; SLE, systemic lupus erythematosus; ssDNA, single-stranded DNA; TREX1, 3′-repair DNA exonuclease 1

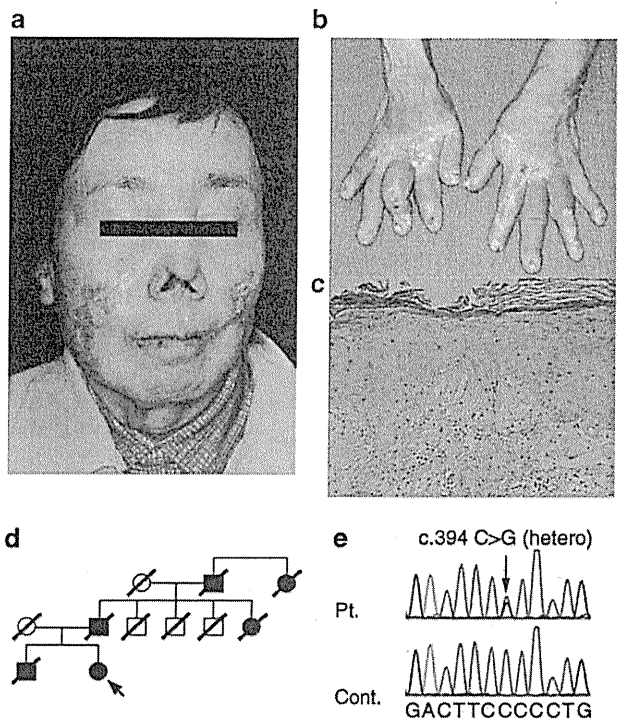

Figure 1. Skin manifestations, pathological tissue, family tree, and *TREX1* DNA sequence data of the patient. (**a**, **b**) Chilblain lesions on the nose, cheeks, lips, hands, and fingertips of the patient. The patient provided written informed consent for publication of photographs. (**c**) Pathological tissue of left hand of the patient. In the upper dermis, the vessel walls appear dilated, and sparse perivascular lymphocytic infiltrations are observed. Basement membrane is thickened. Bar = 50 μm. (**d**) Family tree of the patient; arrow denotes the patient. Square represents male member, and circle represents female member; filled symbols indicate family members with clinical features of familial chilblain lupus. (**e**) Sequence data of TREX1 in the patient and control; arrow shows heterozygous mutation of 394C>G. Pt., patient; Cont., control.

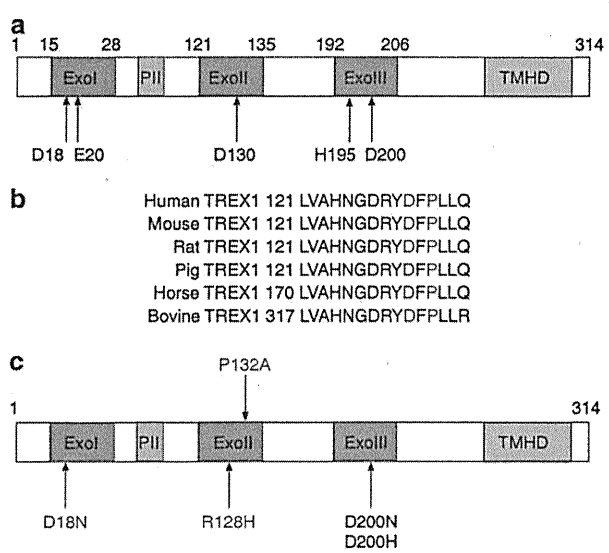

Figure 2. Diagram of TREX1, and alignment of DEDDh exonucleases and human heterozygous missense mutations in the catalytic domain of TREX1. (**a**) Diagram of TREX1. Exo represents exonuclease-conserved motifs, PII the polyproline II motif, and TMHD the transmembrane helix domain. Enzymes from the DEDDh 3′–5′exonuclease superfamily are characterized by five acidic residues (three aspartates (D), one glutamate (E), and one histidine (H)). (**b**) Sequence alignment of Exo II in TREX1. DEDDh motif is indicated in blue, and P132 is in red. (**c**) Human heterozygous missense mutation of *TREX1* identified in the Exos. Black indicates mutations identified in AGS cases; blue indicates mutations in AGS and FCL cases; and purple indicates mutations in neuropsychiatric systemic lupus erythematosus. Red indicates the present case of familial chilblain lupus. All patients have severe chilblain lupus.

exonuclease domains II and III. It is noteworthy that one member of a family with FCL with c.375dupT had no CL or other symptoms even with this mutation. Therefore, the c.375dupT mutation of TREX1 does not always cause CL. Lee-Kirsch *et al.* (2006, 2007a) reported another heterozygous missense mutation, p.Asp18Asn, in *TREX1* in 13 patients in one large family with FCL. It is intriguing that p.Asp18Asn was also detected in an AGS patient showing CL (Haaxma *et al.*, 2010).

In summary, of all cases having heterozygous missense mutations in the three exonuclease domains of TREX1, we found 18 patients available for clinical information, including the present case, with a total of five missense mutations, and all the cases had severe early-onset CL or finger gangrene (Figure 2c). Of the five, three were heterozygous missense mutations, p.Asp18Asn, p.Asp200Asn, and p.Asp200His, which involve key catalytic residues of DEDDh motif, asparatic acids at codon No. 18 and No. 200 directly. The three missense mutations possess significantly reduced exonuclease activity against ssDNA and, in addition, to inhibit wild-type protein activity *in vitro* (Lee-Kirsch *et al.*, 2007a; Lehtinen *et al.*, 2008). The other two mutations, p.Arg128His and p.Pro132Ala, are missense mutations at conserved amino acids adjacent to the DEDDh motif. In addition, we speculate that these mutations have slightly reduced TREX1 exonuclease activity, but inhibit wild-type protein activity by forming dimers of wild-type and mutant.

We also reviewed all heterozygous missense mutations of *TREX1* that are outside of the exonuclease domains. A total of 20 SLE cases with 10 types of heterozygous missense mutations were described, but none of these had CL (Lee-Kirsch *et al.*, 2007b; Namjou *et al.*, 2011).

In conclusion, it is noteworthy that heterozygous missense mutations of DEDDh motif or their adjacent in the exonuclease catalytic domain of TREX1 always lead to severe CL, without exception. Further studies are needed to elucidate the exact mechanisms of how the defective TREX1 activity results in the specific CL phenotype.

CONFLICT OF INTEREST
The authors state no conflict of interest.

ACKNOWLEDGMENTS
This study was supported in part by a Grant-in-Aid for Scientific Research, (C) 23591617 (K.S.) from the Ministry of Education, Culture, Sports, Science and Technology of Japan and by a Grant-in-Aid for Scientific Research, (A) 23249058 (M.A.) from the Ministry of Education, Culture, Sports, Science and Technology of Japan.

Kazumitsu Sugiura[1], *Takuya Takeichi*[1,2], *Michihiro Kono*[1], *Yasuki Ito*[3], *Yasushi Ogawa*[1], *Yoshinao Muro*[1] *and Masashi Akiyama*[1]

[1]*Department of Dermatology, Nagoya University Graduate School of Medicine, Nagoya, Japan;* [2]*Department of Dermatology, Inazawa City Hospital, Inazawa, Japan and* [3]*Department of Ophthalmology, Nagoya University Graduate School of Medicine, Nagoya, Japan*
E-mail: kazusugi@med.nagoya-u.ac.jp

SUPPLEMENTARY MATERIAL

Supplementary material is linked to the online version of the paper at http://www.nature.com/jid

REFERENCES

Brucet M, Querol-Audí J, Serra M *et al.* (2007) Structure of the dimeric exonuclease TREX1 in complex with DNA displays a proline-rich binding site for WW domains. *J Biol Chem* 282:14547–57

Crow YJ, Hayward BE, Parmar R *et al.* (2006) Mutations in the gene encoding the 3′-5′ DNA exonuclease TREX1 cause Aicardi-Goutières syndrome at the AGS1 locus. *Nat Genet* 38:917–20

de Vries B, Steup-Beekman GM, Haan J *et al.* (2010) TREX1 gene variant in neuropsychiatric systemic lupus erythematosus. *Ann Rheum Dis* 69:1886–7

Haaxma CA, Crow YJ, van Steensel MA *et al.* (2010) A *de novo* p.Asp18Asn mutation in TREX1 in a patient with Aicardi-Goutières syndrome. *Am J Med Genet A* 152A: 2612–7

Lee-Kirsch MA, Chowdhury D, Harvey S *et al.* (2007a) A mutation in TREX1 that impairs susceptibility to granzyme A-mediated cell death underlies familial chilblain lupus. *J Mol Med* 85:531–7

Lee-Kirsch MA, Gong M, Chowdhury D *et al.* (2007b) Mutations in the gene encoding the 3′-5′ DNA exonuclease TREX1 are associated with systemic lupus erythematosus. *Nat Genet* 39:1065–7

Lee-Kirsch MA, Gong M, Schulz H *et al.* (2006) Familial chilblain lupus, a monogenic form of cutaneous lupus erythematosus, maps to chromosome 3p. *Am J Hum Genet* 79:731–7

Lehtinen DA, Harvey S, Mulcahy MJ *et al.* (2008) The TREX1 double-stranded DNA degradation activity is defective in dominant mutations associated with autoimmune disease. *J Biol Chem* 283:31649–56

Namjou B, Kothari PH, Kelly JA *et al.* (2011) Evaluation of the TREX1 gene in a large multi-ancestral lupus cohort. *Genes Immun* 12:270–9

Ramantani G, Kohlhase J, Hertzberg C *et al.* (2010) Expanding the phenotypic spectrum of lupus erythematosus in Aicardi-Goutières syndrome. *Arthritis Rheum* 62:1469–77

Rice G, Newman WG, Dean J *et al.* (2007) Heterozygous mutations in TREX1 cause familial chilblain lupus and dominant Aicardi-Goutieres syndrome. *Am J Hum Genet* 80: 811–5

Richards A, van den Maagdenberg AM, Jen JC *et al.* (2007) C-terminal truncations in human 3′-5′ DNA exonuclease TREX1 cause autosomal dominant retinal vasculopathy with cerebral leukodystrophy. *Nat Genet* 39:1068–70

Filaggrin Degradation by Caspase-14 Is Required for UVB Photoprotection but Does Not Influence Allergic Sensitization in a Mouse Model of Atopic Dermatitis

Journal of Investigative Dermatology (2012) **132,** 2857–2860; doi:10.1038/jid.2012.236; published online 30 August 2012

TO THE EDITOR

Filaggrin (filament-aggregating protein) is a major structural component of the cornified envelope, which is crucial for formation of the stratum corneum (SC) barrier. It is synthesized as a large precursor, which is stored in the keratohyalin granules in the granular layer. Upon cornification, filaggrin units are generated by proteolysis and released to promote aggregation of keratin intermediate filaments into macrofibrils (reviewed in Brown and McLean, 2012). During the final cornification steps, filaggrin is degraded into single amino acids by several enzymes. These hygroscopic amino acids, together with their derivatives, are the main components of the natural moisturizing factors (NMFs) needed for hydration of the SC (Scott *et al.*, 1982). We have shown that caspase-14, a unique member of the caspase protease family, can directly cleave the filaggrin monomer *in vitro* (Hoste *et al.*, 2011). Moreover, caspase-14-deficient mice accumulate incomplete filaggrin breakdown products within the SC, leading to reduced levels of NMF and lower SC hydration (Hoste *et al.*, 2011). In addition, transepidermal water loss is increased in these mice, which are also sensitized to UVB photodamage (Denecker *et al.*, 2007).

An important component of the NMFs is *trans*-urocanic acid (*trans*-UCA), a product of histidine deimination by the enzyme histidase. *Trans*-UCA acts as a major chromophore in the skin and is converted by UVB to *cis*-UCA, which has immunomodulatory functions (Gibbs *et al.*, 2008). We hypothesized that the increase in UVB-induced photodamage in caspase-14-deficient mice is the consequence of lower levels of *trans*-UCA in the SC of these mice compared with wild type. This hypothesis is supported by two recent findings: (1) knockdown of filaggrin in a human skin model leads to

Abbreviations: AD, atopic dermatitis; CPD, cyclobutane pyrimidine dimer; filaggrin, filament-aggregating protein; NMF, natural moisturizing factor; OVA, ovalbumin; SC, stratum corneum; trans-*UCA,* trans-*urocanic acid*

The American Journal of Pathology, Vol. 181, No. 5, November 2012

http://dx.doi.org/10.1016/j.ajpath.2012.07.018

Epithelial and Mesenchymal Cell Biology

Type VII Collagen Deficiency Causes Defective Tooth Enamel Formation due to Poor Differentiation of Ameloblasts

Hiroko Umemoto,*† Masashi Akiyama,*‡ Takanori Domon,§ Toshifumi Nomura,* Satoru Shinkuma,* Kei Ito,* Takuya Asaka,† Daisuke Sawamura,¶ Jouni Uitto,‖ Motohiro Uo,** Yoshimasa Kitagawa,† and Hiroshi Shimizu*

From the Departments of Dermatology, Hokkaido University Graduate School of Medicine, Sapporo, Japan; the Departments of Oral Diagnosis and Oral Medicine,† and Oral Functional Anatomy, Division of Oral Functional Science,§ Hokkaido University Graduate School of Dental Medicine, Sapporo, Japan; the Department of Dermatology,‡ Nagoya University Graduate School of Medicine, Nagoya, Japan; the Department of Dermatology,¶ Hirosaki University Graduate School of Medicine, Hirosaki, Japan; the Department of Dermatology and Cutaneous Biology,‖ Jefferson Medical College and Jefferson Institute of Molecular Medicine, Thomas Jefferson University, Philadelphia, Pennsylvania; and the Advanced Biomaterials Section,** Graduate School of Medical and Dental Sciences, Tokyo Medical and Dental University, Tokyo, Japan*

Recessive dystrophic epidermolysis bullosa (RDEB) is caused by mutations in the gene encoding type VII collagen (COL7), a major component of anchoring fibrils in the epidermal basement membrane zone. Patients with RDEB present a low oral hygiene index and prevalent tooth abnormalities with caries. We examined the tooth enamel structure of an RDEB patient by scanning electron microscopy. It showed irregular enamel prisms, indicating structural enamel defects. To elucidate the pathomechanisms of enamel defects due to COL7 deficiency, we investigated tooth formation in *Col7a1*$^{-/-}$ and COL7-rescued humanized mice that we have established. The enamel from *Col7a1*$^{-/-}$ mice had normal surface structure. The enamel calcification and chemical composition of *Col7a1*$^{-/-}$ mice were similar to those of the wild type. However, transverse sections of teeth from the *Col7a1*$^{-/-}$ mice showed irregular enamel prisms, which were also observed in the RDEB patient. Furthermore, the *Col7a1*$^{-/-}$ mice teeth had poorly differentiated ameloblasts, lacking normal enamel protein–secreting Tomes' processes, and showed reduced mRNA expression of amelogenin and other enamel-related molecules. These enamel abnormalities were corrected in the COL7-rescued humanized mice expressing a human *COL7A1* transgene. These findings suggest that COL7 regulates ameloblast differentiation and is essential for the formation of Tomes' processes. Collectively, COL7 deficiency is thought to disrupt epithelial–mesenchymal interactions, leading to defective ameloblast differentiation and enamel malformation in RDEB patients. *(Am J Pathol 2012, 181: 1659–1671; http://dx.doi.org/10.1016/j.ajpath.2012.07.018)*

Mesenchymal–epithelial interactions are thought to play essential roles in the development of epithelial organs, including the epidermis, hair follicles, and teeth. Various soluble factors, cell surface markers, and signal molecules have been reported to be involved in mesenchymal–epithelial interactions.[1,2]

Several mouse models with epithelial mesenchymal junction (EMJ) component deficiencies have been developed.[3] Of these, type XVII collagen (COL17)-deficient mice and laminin332-deficient mice show tooth malformation[4,5] and junctional epidermolysis bullosa (EB) caused by deficiencies of these molecules shows the abnormal tooth formation of amelogenesis imperfecta.[6] COL17 and laminin332 play a crucial role in hemidesmosome stability and epithelial mesenchymal attachment. The teeth of COL17-deficient mice exhibit reduced yellow pigmentation, diminished iron deposition, delayed calci-

Supported in part by Grants-in-Aid for Scientific Research from the Ministry of Education, Science, Sports and Culture of Japan to H.S. (Kiban A, No. 21249063) and M.A. (Kiban A, No. 23249058).

Accepted for publication July 18, 2012.

A guest editor acted as editor-in-chief for this manuscript. No person at Thomas Jefferson University was involved in the peer review process or final disposition of this article.

Address reprint requests to Masashi Akiyama, M.D., Ph.D., Department of Dermatology, Nagoya University Graduate School of Medicine, Tsurumaicho 65, Showa-ku, Nagoya 466-8550, Japan. E-mail: makiyama@med.nagoya-u.ac.jp.

fication, and irregular enamel prisms. Furthermore, poorly differentiated ameloblasts are revealed in COL17-deficient mice. The teeth of laminin332-deficient mice also have remarkable abnormalities, including disturbance of ameloblast differentiation and reduced enamel deposition. These findings indicate that COL17 and laminin332 deficiency disrupts epithelial–mesenchymal interactions, leading to defective ameloblast differentiation and enamel malformation.[4,5] Thus, it is important to study the pathomechanisms of enamel malformation in mice with defects in other basement membrane zone components.

Anchoring fibrils are subcellular adhesion structures in the basement membrane zone just beneath the lamina densa between the mesenchymal and epithelial cells, which bind the epithelial cells to the underlying mesenchymal tissue.[7] Type VII collagen (COL7) is expressed in stratified and complex epithelia, such as the epidermis of skin and the oral mucosal epithelium, and is identified as the major protein component of anchoring fibrils. COL7 plays a crucial role in anchoring fibril formation and mediates dermal–epidermal adherence.[8] Anchoring fibrils consist of a central collagenous triple-helical domain flanked by two noncollagenous, globular domains, the NC1 and NC2 domains of COL7. It was reported that the NC1 domain of COL7 binds laminin332 with high affinity.[9] The NC1 domain binds predominantly to the β3 chain of laminin332, but also to the γ2 chain.[10] We, therefore, hypothesized that COL7 in anchoring fibrils also plays an important role in mesenchymal–epithelial interactions in tooth formation.

Recessive dystrophic epidermolysis bullosa (RDEB), which is caused by COL7 deficiency, shows mucocutaneous blistering in response to minor trauma, followed by milium and scar formation, joint contractures, and strictures of the esophagus.[11] RDEB patients also present with a distinct pattern of oral involvement consisting of microstomia, ankyloglossia, vestibule obliteration, and dental caries.[12,13] It has been speculated in the literature that the tendency of RDEB patients to have higher caries index is due to structural abnormalities of the teeth. However, it is unknown to what extent the apparently high susceptibility to enamel caries in these cases is due to disease-related altered enamel structure or to low oral hygiene owing to blisters and erosions in the oral mucosa. The debate largely subsided after it was demonstrated that the chemical composition of enamel in RDEB patients is normal.[14] Furthermore, it was demonstrated that RDEB patients have enamel surface defects that show similar frequency and distribution to those in healthy controls.[15] Thus, it has been suggested that tooth malposition and the cross-bite relationship between maxilla and mandible could play a major role in promoting enamel caries.[16] Poor oral hygiene conditions can result from the inability to brush the teeth, as tooth brushing is painful and evokes blister formation. This eventually leads to the early onset and severe manifestations of caries. However, it has not been fully elucidated whether the frequent dental caries is due to disease-related structural disruption of the enamel itself or to poor oral hygiene owing to RDEB oral mucosal lesions, because enamel formation is easily disrupted and enamel defects may reflect more than just genetic abnormalities. Enamel defects can also be attributed to environmental factors that cause chronological hypoplasia of the enamel during the enamel formation period.[17] In this context, as a preliminary study, we observed the tooth enamel structure of an RDEB patient and found irregular enamel prisms indicating structural defects of the enamel.

We previously established *Col7a1* knockout (*Col7a1*$^{-/-}$) mice,[18] a potentially useful model for investigations into the pathomechanisms of enamel defects that arise from defects in anchoring fibrils caused by COL7 deficiency. In the present study, to clarify the roles of COL7 in tooth formation, we studied the detailed process of tooth formation in *Col7a1* knockout (*Col7a1*$^{-/-}$) mice.[18]

Tooth development is mediated by reciprocal interdependent epithelial–mesenchymal interactions resulting in the differentiation of epithelial cells into ameloblasts, and mesenchymal cells into odontoblast cells.[19] Enamel formation, known as amelogenesis, is divided into three main stages: i) presecretory; ii) secretory; and iii) maturation. In the presecretory stage, epithelial cells differentiate into ameloblasts. In the secretory stage, ameloblasts synthesize and secrete tissue-specific proteins into the developing enamel extracellular matrix. In the maturation stage, removal of organic components and water from the extracellular matrix is followed by the formation of calcium hydroxyapatite crystals, resulting in conversion of the enamel extracellular matrix to fully mineralized enamel.

We show that COL7 has important roles in tooth formation, especially in enamelization and ameloblast differentiation, suggesting the importance of anchoring fibrils in the mesenchymal–epithelial interaction during tooth formation. In this context, we speculate that the high frequency of enamel caries in RDEB patients might be attributable to enamel malformation caused by the disturbed differentiation of ameloblasts.

Materials and Methods

Analysis of an RDEB Patient's Dentition

We obtained teeth from a 9-year-old female patient with RDEB (Figure 1, A and B). She harbored compound heterozygous mutations in *COL7A1*, c.6574 + 1G>C and c.8109 + 2T>A, described elsewhere.[20] Immunofluorescence staining of skin for COL7 showed that the expression level of COL7 was reduced compared with a normal control (Figure 1, C and D), whereas type IV collagen (COL4) and laminin332, which are the major protein components of the lamina densa and anchoring filaments, respectively, in the EMJ, showed equal brightness at the EMJ in the patient and the normal control (Figure 1, E–H). Dental caries was seen on the enamel surface, although she had dental treatment as soon as tooth eruption occurred. She had presented with microstomia; therefore, the permanent first premolars were extracted to prevent tooth malposition. The extracted premolars were prepared for structural observations as follows. The teeth were carefully cleaned and were observed macroscopi-

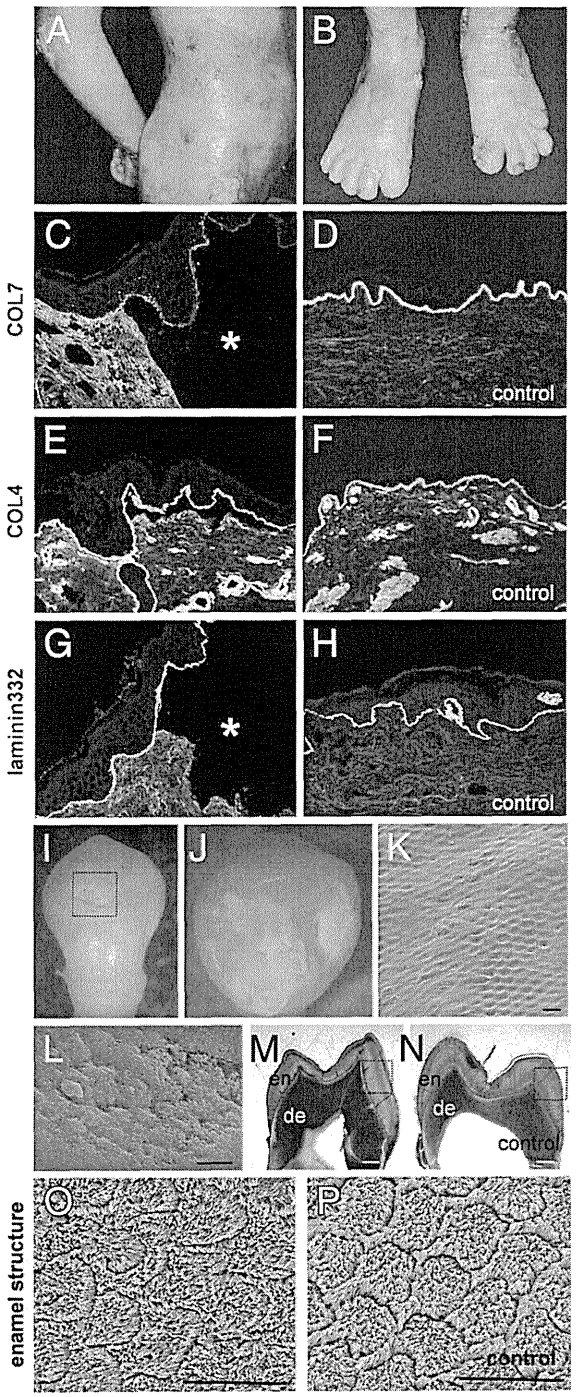

Figure 1. Analysis of the RDEB patient's dentition. **A** and **B:** The RDEB patient with compound heterozygous mutations in *COL7A1* exhibits mucocutaneous blistering in response to minor trauma. **C–H:** Immunofluorescence staining of the patient's skin for COL7 shows reduced expression of COL7 (**C**) compared with the normal control (**D**), whereas type IV collagen (COL4) (**E** and **F**) and laminin332 (**G** and **H**), which are major protein components of the lamina densa and the anchoring filaments, respectively, in the EMJ, show a brightness at the EMJ that is the same in the patient (**E** and **G**) and the normal control (**F** and **H**). Separation between epidermis and dermis (**asterisk**) is seen in the patient's skin (**C** and **G**). **I** and **J:** Dental caries with whitish color is seen on the enamel surface of the permanent premolar (**I:** labial surface, **J:** occlusal surface). **K** and **L:** By SEM, the dental caries, indicated by the **dotted rectangle** in **I**, shows a rough and pitted appearance on the enamel surface of the patient. A high-power view of the enamel surface is seen in **L**. **M** and **N:** The overall structure of the enamel layer is similar in the labiolingual section of the patient's premolar and the healthy control at the light microscopic level. **O** and **P:** Ultrastructurally, in the section of the patient's premolar, the pattern of enamel rods is disrupted in the enamel layer (**O**) in contrast with the healthy control (**P**). Scale bars: 10 μm (**K**); 1 μm (**L**); 1 mm (**M** and **N**); 10 μm (**O** and **P**). de, dentin; en, enamel.

cally. After overnight air-drying, the teeth were sputter-coated with carbon CC-40F (Meiwa-shouji, Osaka, Japan) and observed with a Hitachi S-4000 scanning electron microscope (SEM) (Hitachi Electronics, Tokyo, Japan) operated at 10 kV. For the observation of enamel structure including enamel rods, the teeth were embedded in polyester resin (Rigolic; Ouken Co., Tokyo, Japan). Labiolingual ground sections of both 150-μm and 1000-μm thicknesses were prepared with a rotary diamond saw (Speadrap ML521; Maruto, Tokyo, Japan) and emery papers. The ground sections were etched for 50 seconds in 1 N hydrochloric acid, and the section of 150-μm thickness was processed for H&E staining and observation by light microscopy. The section of 1000-μm thickness was similarly observed with SEM.

Generation of Col7a1$^{-/-}$ *Mice and COL7-Rescued Humanized Mice*

The procedure for generating *Col7a1*$^{+/-}$ mice has been described.[18] The genotype of the *Col7a1*$^{+/-}$ mice was verified by PCR of the *Col7a1* (GenBank accession number U32177) and the *neo* genes with a template of genomic DNA from tail samples. *Col7a1*$^{+/-}$ mice were clinically normal and indistinguishable from their wild-type littermates (*Col7a1*$^{+/+}$). Heterozygous mice were intercrossed to produce *Col7a1*-null (*Col7a1*$^{-/-}$) offspring. The procedures for screening *Col7a1*$^{-/-}$ mice by PCR, Northern and Western blotting, histology, electron microscopy, and immunofluorescence are described elsewhere.[18]

The phenotypic features of the *Col7a1* knockout (*Col7a1*$^{-/-}$) mice closely resemble those seen in RDEB (OMIM: 226600), caused by null mutations in the *COL7A1* gene (GenBank accession number L23982), as previously described.[18] The *Col7a1*$^{-/-}$ mice are readily identified at birth by large, fluid-filled blisters that develop primarily on the ventral side of the animals and by large hemorrhagic blisters on the paws. Skin blisters and erosions readily form from minor trauma. The *Col7a1*$^{-/-}$ mice skin showed the subepidermal blistering associated with a lack of COL7, and the mice entirely lacked ultrastructurally recognizable anchoring fibrils.

Procedures for generating COL7-rescued humanized mice have been described elsewhere.[21] Briefly, we crossed transgenic mice (C57BL/6 background) expressing human *COL7A1* cDNA (*Col7a1*$^{+/+}$, *COL7A1*$^{+}$) driven by the squamous epithelium-specific K14 promoter with heterozygous *Col7a1*$^{+/-}$ mice. Mice that carried both the heterozygous null mutation in *Col7a1* and the transgene of human *COL7A1* (*Col7a1*$^{+/-}$, *COL7A1*$^{+}$) were bred to produce rescued *Col7a1*$^{-/-}$, *COL7A1*$^{+}$ COL7-humanized mice. The rescued mice lacked the abnormal manifestations seen in the *Col7a1*$^{-/-}$ mice.[21] In the COL7-rescued mice (*Col7a1*$^{-/-}$, human *COL7A1*$^{+}$ mice), intact anchoring fibrils are already observed at the presecretory stage of ameloblast differentiation. Thus, the rescue of deficiency in COL7 by the human gene occurs very early in dental development: the presecretory stage or earlier.

Structural Analysis of Mouse Dentition

Tissue samples of mice were incubated in hot (approximately 90°C) distilled water for several minutes and soaked in 10% Tasinase (Kyowa-hakkou, Tokyo, Japan) at 37°C for 6 hours. Incisors and molars were taken from maxillomandibular tissue by removal of soft tissue. The teeth were carefully cleaned and were observed macroscopically. After overnight air drying, the teeth were sputter-coated with carbon CC-40F (Meiwa-shouji) and observed with a Hitachi S-4000 SEM operated at 10 kV. For the observation of enamel rod inclination, incisors were embedded in polyester resin (Rigolic; Ouken Co.). Transverse labiolingual ground sections of 1-mm thickness were prepared with a rotary diamond saw and emery papers. The ground sections were etched for 30 seconds in 0.1 N hydrochloric acid and were observed similarly.

Chemical and Mineralization Analysis

Qualitative and distributive elemental analyses were performed for polyester resin–embedded transverse ground sections of incisors and molars that had been prepared with a rotary diamond saw and emery paper. These analyses were done using a Hitachi S-2380 SEM, operated at 15 kV, and energy-dispersive X-ray spectrometry.

To demonstrate the patterns of mineralization, microcomputed tomography (CT) scanning was performed using an R_mCT2 (Rigaku, Tokyo, Japan). The maxillae and mandibles with incisors were obtained and dehydrated by passage through a series of ascending concentrations of ethanol solution before being embedded in polyester resin. The samples were placed longitudinally into a sample holder for CT scanning. The scanning protocol was set at an X-ray energy setting of 90 kV and 160 μA performed for one full 360° rotation. From the scans, a three-dimensional reconstruction of the sample was made using software supplied with the scanner, resulting in datasets with an isotropic voxel size of 20 μm.

Preparation of Tissue Sections and Immunohistochemistry

Under anesthesia with ether inhalation, intracardiac perfusions of the mice were performed with a fixative solution containing 4% paraformaldehyde in PBS, at pH 7.4. Postfixation was ensured by immersion of the dissected maxilla and mandible in the fixative solution overnight at 4°C.

The maxillae and mandibles with incisors and molars were processed for histological analysis by decalcification at 4°C for up to 2 weeks in PBS solution (pH 7.4) containing 5% EDTA. After extensive washing in PBS, the samples were dehydrated in increasing concentrations of ethanol and Lemosol (Wako, Osaka, Japan) before being embedded in paraffin. Serial longitudinal sections of the incisors of the paraffin-embedded specimens (5 μm) were processed for H&E staining and for Berlin blue staining to detect iron deposits.

For immunohistochemistry, neonatal mice were sacrificed and the tissue samples were embedded in optimal cutting temperature compound (Sakura Finetechnical Co., Tokyo, Japan) for frozen sectioning. Frozen tissue sections were cut sagittally to a thickness of 6 μm until incisors and molars were exposed. After air drying for several minutes, sections were washed in PBS and incubated with a primary antibody—either anti-mouse COL7 polyclonal antibody (Calbiochem, Darmstadt, Germany; final dilution of 1:200), anti-mouse COL4 polyclonal antibody (Abcam, Cambridge, UK; final dilution of 1:400), or anti-mouse laminin332 polyclonal antibody (Abcam; final dilution of 1:50)—at 37°C for 30 minutes. The sections were then incubated with a secondary antibody—fluorescein isothiocyanate (FITC)-conjugated goat anti-rabbit IgG (H+L; Jackson ImmunoResearch Laboratories, Newmarket, UK; final dilution, 1:50, 1:200, 1:50)—at 37°C for 30 minutes and incubated with 10 μg/mL of propidium iodide at 37°C for 10 minutes for nuclear counterstaining. Sections were observed under an Olympus Fluoview confocal laser-scanning microscope (Olympus, Tokyo, Japan).

Ultrastructural Analysis during Tooth Formation

As above, mice incisors and molars were obtained from the maxillomandibular tissue fixed with modified Karnovsky's fixative [final concentration of 2% paraformaldehyde and 2.5% glutaraldehyde in 0.05 mol/L cacodylate buffer solution (pH 7.4)], and decalcified in 5% EDTA (pH 7.4) at 4°C for 2 weeks. After decalcification, samples were postfixed in 1% osmium tetroxide at 4°C for 2 hours and stained *en bloc* with 1% uranyl acetate at 4°C for 20 minutes. The samples were dehydrated through a graded series of ethanol and embedded in Epon 812 (TAAB Laboratories, Aldermaston, UK). Ultrathin sections were cut in the sagittal direction to include both the separated enamel organ and the dental papilla. Sections were stained with uranyl acetate and lead citrate, and observed under a Hitachi H-7100 transmission electron microscope.

Cell Cultures and Immunolabeling

For dental epithelial cell cultures, maxillary and mandibular incisors and molars from mice were dissected. Tooth samples were treated with 0.25% trypsin for 10 minutes and pipetted up and down intensely. Dental epithelial cells, dental mesenchymal cells and various other cells were isolated from tooth buds. To separate dental epithelial cells from the other cells, the cells were cultured in epidermal keratinocyte medium containing a small amount of bovine pituitary extract (CnT-57; CELLnTEC Advanced Cell Systems, Bern, Switzerland) for 7 days. After obtaining a sufficient number of dental progenitor epithelial cells, we changed the culture medium to epidermal keratinocyte medium containing 0.07 mmol/L calcium (CnT-02; CELLnTEC Advanced Cell Systems) to induce differentiation, and cultured the cells for 10 days.

For fluorescence staining, the cells were fixed with 70% ethanol for 10 minutes and washed with PBS. The cells were incubated with a primary antibody anti-mouse amelogenin polyclonal antibody (Hokudo, Sapporo, Japan), final dilution of 1:100, or with anti-mouse ameloblas-